THEMA
théorie économique, modélisation et applications

THEMA Working Paper n°2023-09
CY Cergy Paris Université, France

# Assessing the Economic Costs of Road Traffic-Related Air Pollution in La Reunion

R. Le Frioux, A. de Palma, N. Blond

May 2023

# Assessing the Economic Costs of Road Traffic-Related Air Pollution in La Réunion

R. Le Frioux[1], A. de Palma[1], N. Blond[2]
[1] CY Cergy Paris Université and ThEMA
[2] Université de Strasbourg, CNRS, Laboratoire Image Ville Environnement, UMR7362, Strasbourg, France

**May 2023**

Working Paper

Key words: dynamic traffic simulation, air pollution, road traffic pollution, population exposure costs, integrated chain of models, electric vehicles,

**ABSTRACT :** *This research builds an integrated chain of models to compute the economic costs of population exposure to air pollution from roads. The framework uses data with a high geographical resolution (1 km x 1 km), a mobility module to simulate population movements, and a Gaussian dispersion model-based exposure model to evaluate population air pollution exposure and the related costs. This paper investigates the impact of two policies on La Réunion, a French island.: replacing old vehicles with electric ones and allowing flexible departure times for commuting trips.*

**Acknowledgment:**

The authors extend their gratitude to all the participants of the AFFINITE seminar for their valuable feedback, as well as to those who participated in the internal seminar of CY Paris Cergy Université. They wish to specifically acknowledge Lindsey Robin, Javaudin Lucas, Ghoslya Samarth, Chapelle Guillaume, and Riou Yannik for their support and insightful comments. Authors are also grateful to MAAT and AFFINITE project for their financial supports.

**JEL :**

I18 – L91 – L92 – P25 – R41 – Q5

## 1. Introduction

Air pollution has important consequences on both environment and health. Through the greenhouse gases (GHG), air pollution has an impact on global warming, which became one of the major problems for our civilizations. Other air pollutants, emitted and formed in the atmosphere, have direct impacts on population well-being and health. According to the World Health Organization, over 99% of the world's population is living above its recommended health protection levels. Air pollution leads each year to 4.2 million premature deaths worldwide in 2017[1]. According to estimates made in Europe, air pollution causes 311,000 premature deaths annually[2]. As reported by Maguire et al. (2020), the top health risk in Europe in 2017 is air pollution. The French Ministry of Ecology and Social Cohesion claims that air pollution causes 48,000 premature deaths annually which represents 9% of the total deaths[3]. In urban areas, the air pollution exhibits the highest levels of air pollution with very diverse distribution over both time and space (Dons et al., 2011; Hatzopoulou and Miller, 2010; Hao, Hatzopoulou, and Miller, 2010; Dhondt et al., 2012; Lefebvre et al., 2013; Rowangould, 2015; Vallamsundar et al., 2016). Several studies detail the impacts of air pollution in several cities on health.[4] Garrett and Casimiro (2011) studied the air pollution in Lisbon, Portugal, focusing particulate matter (PM) and on ozone ($O_3$). They found that when PM levels increased by 10 $\mu g.m^{-3}$, the risk of cardiovascular mortality for individuals over 65 years old increased by 2.39%. They also found that $O_3$ caused a 1.1% increase in all-cause mortality and a 0.96% for the same age group. Bañeras et al. (2018) looked at the short-term correlation between air pollution and cardiovascular disease and mortality in the Barcelona region in Spain. They found that when PM levels increased by 10 $\mu g.m^{-3}$, mortality increased by 1.06% and cardiovascular illnesses increased by 1.015%. In a sample of 74 cities in China, Fang et al. (2016) studied the impact of fine PM pollution on health. They found that in 2013, 20% of reported deaths were due to cardiovascular, respiratory, and lung cancer causes, and 32% were related to $PM_{2.5}$. Studies have shown that increased levels of nitrogen dioxide ($NO_2$) are associated with increased rates of mortality and hospitalization for respiratory and cardiovascular illnesses. For example, a study conducted by Faustini et al. (2010) found that an increase of 10 $\mu g.m^{-3}$ in $NO_2$ levels was associated with a 3% increase in all-cause mortality.

These health consequences have very significant social costs. Many studies in the epidemiological literature have estimated costs for various pollutants and different cities. The death burden of PM and $NO_x$ concentrations was computed by Walton et al. (2015). In 2010, they estimated that the economic expenses associated with the health effects of PM and $NO_2$ ranged from 1.4 to 3.7 billion pounds for the London area. Vlachokostas et al. (2012) conducted a study on Thessaloniki great area (Greece), where they estimated the social costs of particulate matter (PM) and ozone (O3) to be around 1,450 million euros, equivalent to 10% of the region's GDP. Between 2005 and 2013, Martinez et al. (2018) computed that Skopje's (Macedonia) overall social cost was between 1,140 and 2,100 million euros annually. Using a sample of 76 European cities, CE Delft (2020) concluded that the average cost of population exposure to pollution in France was approximately 10,953 million euros, with an average cost per person of 943 euros, ranging from 467 euros for Pau to 1,602 euros for Paris. They also demonstrated that, on average, PM are the most dangerous pollutants, accounting for roughly 80% of total expenses, followed by $NO_2$, which accounts for 15%. $CO_2$ has a high societal cost since it causes global warming even if it is not harmful to human health. The World Bank estimates that the social costs of $CO_2$ were roughly 300 dollars per resident worldwide and 100 in France in 2019[5].

Indeed, road transportation is a significant contributor to air pollution and a major public health concern since people are more likely to be exposed to it due to their proximity to roads or their reliance on cars for transportation (McCubbin and Delucchi, 2003). In 2020, the European Environment Agency estimates that road transportation contributes to around 70% of the total European emissions from the transportation sector. It accounted also for 37% of $NO_x$ emissions, 18% of CO emissions, and 9% of $PM_{2.5}$ emissions. According to a report of the International Energy Agency, the transportation sector is responsible for approximately one-quarter of total energy-related $CO_2$ emissions globally[6]. In Europe in 2017, 27% of total GHG came from the transport sector (22% if international aviation and maritime emissions are excluded)[7].

Xie et al. (2017) proposed a recent review of urban air pollution monitoring and exposure assessment methods. Most studies related to road traffic have been performed using road and traffic data collected from diverse modelling systems. These traffic data are used to compute traffic air pollutant emissions and/or as external predictor variables to better

1 https://www.who.int/news-room/fact-sheets/detail/ambient-(outdoor)-air-quality-and-health

2 https://www.eea.europa.eu/highlights/premature-deaths-due-to-air

3 https://www.ecologie.gouv.fr/pollution-lair-origines-situation-et-impacts (in French)

4 For a more exhaustive summery ttps://www.eea.europa.eu/themes/air/health-impacts-of-air-pollution

5 https://data.worldbank.org/indicator/EN.ATM.CO2E.PP.GD.KD

6 https://www.iea.org/reports/transportation-sector-emissions

7 https://www.eea.europa.eu/publications/air-quality-in-europe-2022/sources-and-emissions-of-air

predict the spatial and temporal variability of the air pollution. Only few other studies describe integrated chains of models (Carslaw & Beevers, 2002; Lim et al., 2004, Gulliver & Briggs, 2004, Dons et al., 2011; Kickhöfer and Kern, 2015 ; Dias et al., 2015; Cesaroni et al., 2015) that cross traffic, air pollution and population exposure. These integrated chains of models have different types. Some systems are based on the use traffic count data (e.g. Carslaw & Beevers, 2002 ; Lim et al., 2004, and Cesaroni et al., 2015), and others on traffic simulation models (e.g. Gulliver & Briggs, 2004; Dons et al., 2011 ; Kickhöfer and Kern, 2015 ; Dias et al., 2015). Contrary to the first ones, the seconds allow dynamic simulations of the traffic and evaluation of transportation policies. Nevertheless, as theoretical representations of the reality, they are uncertain and must be validated using observed data. Some studies provide information on pollutant concentrations (e.g. Carslaw & Beevers, 2002 ; Lim et al., 2004 ; Dias et al., 2015) while others include also a population exposure model in their chain (e.g. Gulliver & Briggs, 2004 ; Dons et al., 2011 ; Kickhöfer and Kern, 2015 ; Cesaroni et al., 2015).

This paper aims first to present a new integrated model enable to assess in a coherent way the traffic volume, speed, and flow on roads, estimate the amount of pollutants emitted by vehicles, forecast the dispersion of pollutants in the air, and estimate the exposure of the population to air pollution, and the associated economic costs. We decided to use a traffic simulation model to assess the effectiveness of different transportation policies before they are put into place, such as fleet restrictions, low-emission zones, toll roads, and traffic restrictions. A specific attention is brought to improve the evaluation of population's spatial and temporal distributions. This evaluation is based using the results of our traffic simulation model, and allow assessing changes in population exposure as a result of changes in concentrations and/or population location. Economic costs of population exposure to pollutants are also computed. These both propositions enable a new evaluation of transportation policies, associated with the a cost-benefits analysis of the air pollution reduction.

Second, the paper aims to present an application of the integrated model to evaluate several mechanisms of public policies. An application of the proposed chain of models is focusing on the analysis of the road-traffic air pollution in La Réunion, a French island. This case study was chosen due to its compact size, its isolation from other areas, and the scarcity of studies conducted on this region. Our objective is to evaluate scenarios aimed at reducing carbon dioxide ($CO_2$) emissions and the population's exposure to traffic-related pollution in La Réunion. In this study, we focus on three pollutants dangerous for health: nitrogen oxides ($NO_x$), carbon monoxide (CO), and particulate matter ($PM_{2.5}$).

Among many possible measures, we decided to evaluate one technical and one non-technical measures. The technical measure concerns the replacement of thermal vehicles with electric vehicles (EVs). We compute elasticities of population exposure costs and emissions, which measure the response in emission when the fraction of EVs is increased (formally, elasticity is the percentage change associated to a 1% switch to EVs). For extrapolating the potential advantages of such actions in the future, these elasticities are useful. Decision-makers can use this information to identify the most efficient methods for lowering emissions and advancing a cleaner, more sustainable transportation system. The paper also examines a non-technical measure that consists in allowing employees more scheduling flexibility.

The paper is organized as follows. Section 2 provided an overview of several technical and non-technical measures that were previously studied. Our integrated chain of models is described in Section 3. The various data that were used in our research are introduced and described in Section 4. The application of this framework on La Réunion (France) is presented in Section 5. Section 6 examined various road traffic regulations. Section 7 concludes and presents future research along with potential improvements.

## 2. Technical and non-technical measures to reduce road-traffic air pollution

To successfully address the problem of road pollution, a complete strategy that incorporates both technical and non-technical solutions is required, since this last handles the issue from multiple perspectives.

Technical measures refer to measures that aims reducing the emission factors using cleaner technologies, such as the use of new lighter vehicles, improving fuel injections, filters, etc, in individual vehicles (D'Elia et al., 2009). They were intensively studied and implemented and are now qualified as not sufficient to address the local and global air pollution issue (D'Elia et al., 2009). Introduction of EVs in the vehicle fleet is a new technical challenge and a significant step

towards reducing the negative impacts of transportation on the environment and public health. Requia et al. (2018) proposed a review in which they noted that most of studies are focusing on PM and conducted in China and the United States. The shift to EVs could bring significant benefits in terms of reducing air pollution, especially in cities where air quality is a major concern since EVs do not emit directly harmful gaseous pollutants in the atmosphere (linked to exhaust and fuel evaporation emissions for thermal vehicles). Indeed, the air pollutant emissions are reduced to the PM emissions due tyre, brake wear and road abrasion, and indirect emissions due to the production processes of the EVs and the electricity generation. The electricity used to charge the batteries must be generated from low-carbon sources for EVs to have the lowest carbon footprint compared to conventional vehicles. With different energy mix over the world, the impacts of EVs on environment have notable regional variances. In our study, we looked at the effects of switching from conventional to EVs on GHG emissions as well as health-harming pollutants including $PM_{2.5}$ for France and especially for La Réunion which has not been studied.

Non-technical measures, on the other hand, refer to measures that reduce the activity of the source, such as road rationing, reduced road capacity, increased public transportation options, reducing the speed or number of vehicles on the road, or promoting alternative modes of transportation, etc (D'Elia et al., 2009). It is significant to note that non-technical measures have been more recently investigated. Numerous public measures are being adopted in cities with the goal of reducing road pollution and population exposure to it. Supply-side measures like increasing urban rail transportation (Adler & van Ommeren, 2016; Gonzalez-Navarro & Turner, 2018; Gu et al., 2021), road rationing (de Grange & Troncose, 2011; Gallego et al., 2013; Kornhauser & Fehlig, 2003, Holman et al., 2015; Wolff, 2014; Margaryan, 2021; Bok et al., 2022), or reducing road capacity (Bou Sleiman, 2022; Kang & Cervero, 2009; Pool Jr & Orski, 2000) have been adopted by policymakers. These investigations, nevertheless, are carried only after the measure has been implemented in the territory. Road pricing appears to be a highly powerful technique to internalize externalities according to the polluter pay principle (Kickhöfer & Kern, 2015; Liu and McDonald, 1999; Santos et al., 2008; Tirachini & Hensher, 2012; Winston & Lander, 2006) (see Vosough et al. (2022) for a more thorough literature analysis), and gasoline taxes (Raeissi et al., 2022), while there is still some social and legal resistance to these kinds of regulations[8]. The demand-side perspective also calls for policies that allows early morning and later evening shopping (Dons et al., 2011). In addition, studies about the impact of teleworking (Elefthrios, 2018; Mokhtarian & Varma, 1998; Shafizadeh et al., 1998; Bamister & Marshall, 2000; Pflueger et al., 2016; Pérez et al., 2004) and carpooling (Delle Site et al., 2022; Meyer, 1999; Xu et al., 2015; Bahat & Bekhor, 2016; Zhu et al., 2016; Li et al., 2017; Wang et al., 2018) should be mentioned. Our study proposes to evaluate the effectiveness of providing employees with more flexibility with respect to their work schedules. This approach has a very low social cost (Henrickson and Kocur 1981) —almost none— which makes it potentially highly interesting and should be widely embraced by the general public.

## 3. A new integrated chain of models to evaluate transportation policies based on their impact on air pollution

An integrated chain of models brings together a range of data and models, each provides different types of information, to form a complete picture of the problem. Our integrated chain of models is expected to give in a coherent way, traffic flows, vehicle speeds, air pollutant emissions, population exposure to air pollution and costs related to this exposure. It also provides information to guide decisions and policies designed to reduce emissions and improve air quality.

Our integrated chain of models has been built following recommendations of Friedrich & Quinet (2011). It is represented in Figure 2 and each of its modules are described in the following sections.

8 This red caps (bonnets rouges) and yellow vests (gilets jaunes) movements in France

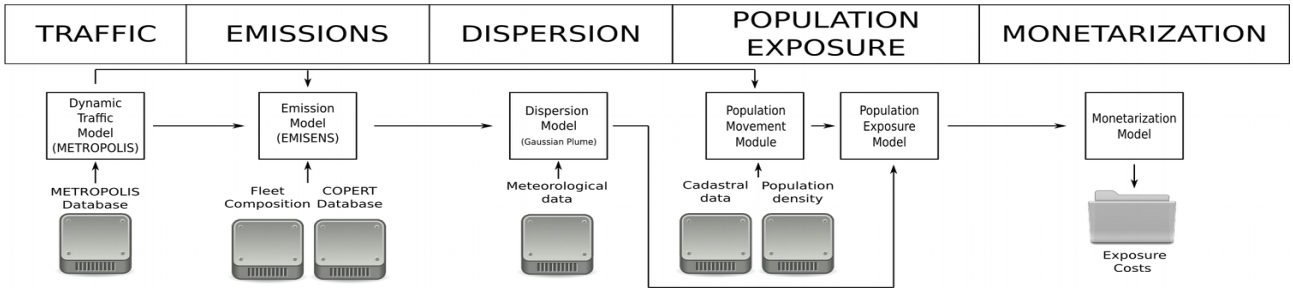


***Figure 1 Graphics of structure of the integrated chain of model, METRO-TRACE (Traffic Related Air pollution Costs Evaluation).***

### 3.1. Road traffic model

Like in Kickhöfer & Kern (2015), Dons et al. (2011), Gulliver & Briggs (2004), and Dias et al. (2015), we chose to use a traffic model in order to explore a wider range of scenarios and policies that could impact pollutant emissions and population exposure to air pollution.

METROPOLIS (de Palma et al., 1997; de Palma & Marchal, 2002) is used. METROPOLIS is a dynamic, mesoscopic[9], traffic simulation model that treats agent-level endogenous options for modes, departure times, and routes.

Using Vickrey (1969) approach, METROPOLIS assumes that every traveller has a cost associated with their preferred schedule for their trip. This cost considers the traveller's desired arrival time and the duration of the trip. The cost is expressed as a function of two components: the deviation from the preferred arrival time and the deviation from the preferred trip duration. Travellers generally prefer to arrive at their destination close to their preferred arrival time and to have a quick trip. This preference can be summarized by the following formula:

$$CA(\tau) = \alpha T(t) + \beta max\left[t^* - \Delta - \tau - T(\tau); 0\right] + \gamma\, max\left[\tau + T(\tau) - t^* - \Delta; 0\right],$$

where $CA(\tau)$ is the systematic cost of departing at time $\tau$, $T(\tau)$ is the travel time, $\alpha$ is the unit cost of travel time, $t^*$ is the desired arrival time, $\Delta$ is the half-width of an on-time arrival window, $\beta$ is the unit costs of arriving early, and $\gamma$ is the unit costs of arriving late.

According to a genetic learning process that considers the situation seen over the previous days, agents review their mode choice, departure time, and route decision each day (de Palma & Marchal, 2002). The system converges to a stationary state as a result of this process. The congestion is modelled using a bottleneck congestion technology (Arnott et al., 1993). This technology assumes that congestion occurs when the rate at which travellers arrive at the bottleneck exceeds the maximum number of travellers that can be accommodated. In this case, travellers are forced to wait in line until they can be processed, resulting in increased travel time and reduced efficiency.

### 3.2. Emissions model

Since precise time variation of the speed profiles are not computed by METROPOLIS, we have adopted a mesoscopic emission model (as defined by Smit et al. 2010) that computes emissions by using emission factors considering the average speed over a defined time period (here 2 minutes) on each link of the studied domain. We used an updated version of the EMISENS model (Ho et al., 2014). According to average speed, ambient outdoor temperature, and traffic volume, EMISENS generates pollutant emissions for four types of air pollutants (in g): nitrogen oxide ($NO_x$), carbon monoxide (CO), particulate matter with diameter lower than 2.5 µm ($PM_{2.5}$), and carbon dioxide ($CO_2$). It allows the computation of hot and cold (excess emissions from a cold engine) emissions from the exhaust pipe. Non-exhaust emissions, such as emissions from tire wear, brake wear, and road abrasions, are also taken into account.

The methodology follows the European EMEP/EA approach. The hot emission factors, $e_k^{hot}\left[S(r_i,t), v\right]$ of pollutant $k$ ($NO_x$, CO, $PM_{2.5}$, or $CO_2$) were collected for each type of vehicle $v$, from the 2019 COPERT database (Ntziachristos et al., 2009) as a function of the vehicle speed $S(r_i,t)$ of directed road $r_i$ during time step $t$. Average emissions factors $\bar{e}_k[S(r_i,t)]$ are based on the fleet composition. It is essential to consider the most updated fleet composition from the area studied or at least from the country (here France). In this paper, we made use of CITEPA's 2019 fleet composition

data. At each time step $t$, the vehicle fluxes (in veh. km) on each directed road $r_i$ evaluated by METROPOLIS are used to compute the activity on each directed road:

$$A(r_i,t)=L(r_i)\times N(r_i,t),$$

where $L(r_i)$ is the length (in km) of directed road $r_i$ and where $N(r_i,t)$ represents the number of residents driving on directed road $r_i$ during time step $t$.

The quantity of pollutant emitted (in g) on directed road $r_i$ during time step $t$, considering that all vehicles have warms engine, is given by the following equation:

$$E^{hot}(r_i,t)=A(r_i,t)\times\bar{e}_k^{hot}\left[S(r_i,t)\right],$$

where $\bar{e}_k^{hot}\left[S(r_i,t)\right]$ denotes the average hot emissions factor according to speed on directed road $r_i$ at time step $t$.

The cold emissions (in g) are emissions to be added to the hot emissions in order to consider that percentage of the driving vehicles have cold engines (just started). Cold emissions are derived from hot emissions using this equation:

$$E_k^{cold}(r_i,t,T_a)=B_k\times E_k^{hot}(r_i,t)\times\left[\frac{\bar{e}_k^{cold}\left[S(r_i,t),T_a\right]}{\bar{e}_k^{hot}\left[S(r_i,t)\right]}\right],$$

where $\bar{e}_k^{cold}\left[S(r_i,t),T_a\right]$ is the average cold emission factor for pollutant $k$ for temperature $T_a$ (in celsius degrees) according to speed on directed road $r_i$ at time step $t$, and $B_k$ is the fraction of vehicles kilometers driven with a cold engine or the catalyst operated below the light-off temperature for pollutant $k$.

The emissions (in g) from tyre wear, brake wear, and road abrasion for directed road $r_i$ during time step $t$ are computed as follows:

$$E_k^{non-exhaust}(t,r_i)=A(r_i,t)\times\left[e_k^{bw}f_k^{bw}+e_k^{rs}f_k^{rs}+e_k^{tw}f_k^{tw}\right],$$

where $e_k^{bw}$ is the emission factor for emissions from brake wear and where $f_k^{bw}$ is the size distribution of brake wear particles for pollutant $k$, $e_k^{rs}$ is the emission factor for emissions from road surface wear and $f_k^{rs}$ is the size distribution of road surface wear particles for pollutant $k$, and $e_k^{tw}$ is the emission factor for emissions from tyre wear and $f_k^{tw}$ is the size distribution of tyre wear particles for pollutant $k$.

Finally, the quantity of pollutant released during one second at emitter $j$ during period $h$ is computed using the following formula:

$$Q_k^j(h)=\sum_{t\in h}\left[\sum_{r_i\in I(j)}\epsilon^j(r_i)\times\left(E^{hot}(t,r_i)+E^{cold}(t,r_i)+E^{non-exhaust}(t,r_i)\right)\right]\times10^{-6}\times\Delta h^{-1},$$

where $\epsilon^j(r_i)$ is the proportion of the directed road $r_i$ included in the cell of the emitter $j$, where $\Delta h$ is the duration of the period $h$ measures in seconds (here 3600), and $I(j)$ is the set of directed road crossing cell $j$.

### 3.3. Dispersion model

Air quality models are numerous, characterized by their numerical approach, their spatial and time resolution linked to the processes simulated and the extension of the domain, and associated computation durations. As in Kickhöfer & Kern (2015), we choose to use a Gaussian model (Sutton, 1947) to mainly focus our study on primary pollutants. Such a model does not compute the chemistry processes (and thus the production of secondary pollutants), and neither the air flow. Nevertheless, it is capable of simulating the dispersion of the air pollution due to the advection of air pollution by the wind considering the air mixing due to the air turbulence, in computationally efficient way. The emissions are given as inputs to a Gaussian plume model to compute the pollutant concentrations.

The emitted air pollutants are dispersed across space based on the distance between the emitter (i.e., the place where the pollutant is discharged) and a receptor, which represents the position of a potential resident. The resulting concentrations is computing as follows:

$$C_k^i(h,(x,y,z)) = \frac{Q_k^j(h)}{2\pi u_s \sigma_y(x)\sigma_z(x)} \exp\left(\frac{-y^2}{2\sigma_y^2(x)}\right)\left[\exp\left(\frac{-(z+H)^2}{2\sigma_z^2(x)}\right)+\exp\left(\frac{-(z-H)^2}{2\sigma_z^2(x)}\right)\right],$$

where $C_k^i(h,(x,y,z))$ (in µg.m$^{-3}$) is the concentration of pollutant $k$ at receptor $i$ during period $h$ with Cartesian coordinates $(x,y,z)$ where $x$ is the downwind distance (in m), $y$ the cross wind distance (in m), $z$ the receptor height (in m). $Q_k^j(h)$ is the quantity of pollutant $k$ released at the emitter $j$ (in µg.s$^{-1}$) during period $h$, $u_s$ is the mean wind speed (in m.s$^{-1}$) at the pollutant release height $H$ (in m). and, $\sigma_y^2(x)$ and $\sigma_z^2(x)$ are the standard deviations of respectively lateral and vertical concentration distribution, also referred to the stability atmospheric parameters. Concentrations are computed for each hour using a grid of receptors with a definition of 100 m. The values of the parameters are dependent of the meteorological conditions of the studied territory. They will be discussed for the case of La Réunion in Section 4.4.

### 3.4. Population exposure model

The population exposure is computed considering that the population is moving in a field of pollutant concentrations greatly varying over space and time, following the proposition of Kickhöfer & Kern (2015), Gulliver & Briggs (2004), and Dons et al. (2011). This exposure model is based on the outputs of the traffic model. Population data issued from are spatialized on a grid domain with a resolution of roughly 1 km$^2$. The module assigns residents at their starting zone based on the density of residential buildings, and at their destination zone based on the density of working buildings. That is, the residents start their journey at their residential cell, and end their journey at their workplace cell. The location of the residents is derived from the METROPOLIS traffic simulation's outputs with a time resolution of one hour for each cell of the grid. In this version, we ignore variations of the exposition during the trip, that is kept to its home value during the trip.

The spatial and temporal distributions of the population are then crossed with the results of the dispersion model that provide the spatial and temporal distributions of the pollutant concentrations to determine the population's exposure to pollutants in each grid cell. According to both the population density in each cell and the average concentration of each pollutant with a spatial resolution of around 1 km$^2$ and a temporal resolution of 1 hour, the exposure to pollutant $k$ in cell $m$ during period $h$ is computed as:

$$\hat{E}_k^m(h) = \bar{C}_k^m(h) \times Pop^m(h),$$

where $\bar{C}^m(h)$ is the hourly average concentrations (in µg.m$^{-3}$) of pollutant $k$ observed in cell $m$ during period $h$ and $Pop^m(h)$ is the population in cell $m$ during period $h$.

### 3.5 Monetarization model

The estimation of the costs of air pollution exposure is a complex, multifaceted and interdisciplinary task that requires considering a wide range of parameters: the air pollution exposure, the health impacts (that are depending on the individual physical characteristics – sensitivity or not to air pollution influencing by socio-economic and environmental context, such poverty, noise, etc.), the impacts on environment (natural ecosystems, biodiversity, resources, buildings, etc.), and the costs associated to these impacts. Both health or environmental impacts could have short and long-term consequences. Since these health impacts can range from respiratory problems with a graduate severity from allergies (can affect a person's ability to work without any use of medicine), asthma, emphysema, cardiovascular diseases, cancer, death (Almetwally et al., 2020). The costs associated with such health impacts can vary widely depending on the financial resources needed to treat the health problems (medical expenses due to interview, analyses and treatments), their consequences (lost workdays, reduced productivity, etc.), or the life cost.

One method used to estimate the costs of pollution-related illness and death is to assign a monetary value to these impacts. This process, known as "valuation" involves assessing the monetary impact of pollution-related health conditions based on factors such as medical expenses, lost workdays, and reduced productivity. Valuing premature deaths caused by air pollution can be particularly challenging, given the complex ways in which air pollution contributes to mortality rates and to the degradation of the quality of life. However, these costs can help policymakers

understand the financial and economic impact of pollution exposure. Short and long-term damages on ecosystems, wildlife, and natural resources are estimated considering factors like the cost of environmental remediation and restoration, the estimated value of ecosystems and biodiversity. By using approaches like valuation and cost-benefit analysis, policymakers can better understand the monetary and economic implications of air pollution and make informed decisions about how to mitigate its negative effects.

In this paper, we adopt a conservative approach. Our costs of population exposure only depend on the expected lives lost. Therefore, our estimates should be viewed as a lower bound of the total costs of pollution. These monetary cost (in \$) of population exposure to pollutant $k$ in cell $m$ during time period $h$ is calculated as follows:

$$€_k^m(h) = \widehat{E}_k^m(h) \times c_k,$$

where $c_k$ is the marginal exposure costs per hour (in \$/µg.m$^{-3}$/inh.).

Since population exposure is computed at a spatial resolution of 1 km$^2$ and a temporal resolution of one hour, our economic model can compute the costs of population exposure with the same level of detail. This results in a highly detailed map of population exposure to pollutants, which can be used by policymakers and public health professionals to identify areas where individuals may be at risk of exposure to harmful pollutants. Such results are also usefull to take appropriate measures to prevent the negative impacts of air pollution.

Additionally, the model provides the opportunity to perform cost-benefit analyses of public policies designed to reduce or prevent exposure to harmful pollutants. By using the information provided by the detailed map of population exposure, policymakers can evaluate the economic benefits of different policy options and make more informed decisions regarding environmental protection and public health.

## 4. Data collection over La Réunion (France) and treatments

This section introduces La Réunion and the data used for analysis. Publicly available data is used for transparency and reproducibility, allowing for collaboration and knowledge sharing. This leads to better policy decisions and outcomes for communities and the environment.

### 4.1. La Réunion

The French island of La Réunion, located in the Indian Ocean, is the focus of this study (as shown in Figure 1). Despite its size and lack of prior research, La Réunion provides a unique opportunity to study mobility driven solely by the local population due to its isolated geography. The transportation network in La Réunion is known for being heavily congested and a major contributor to air pollution. The INSEE (Coudrin and Mariotti, 2020) reported that from 2004 to 2017, residents of La Réunion produced 6 tons of $CO_{2eq}$ (carbon dioxide equivalent) per year, with transportation accounting for 40% of the island's $CO_2$ emissions in 2017 and 88% of that amount being due to road traffic. In 2019, 66% of commutes in La Réunion were made by car and this number increased to 79% for commutes to work. The average travel distance in 2020 was 11 kilometers, which had increased by 10% over a ten-year period. Thus, while La Réunion has already taken steps to improve its fleet, more work is needed to reduce its impact on the environment and population.

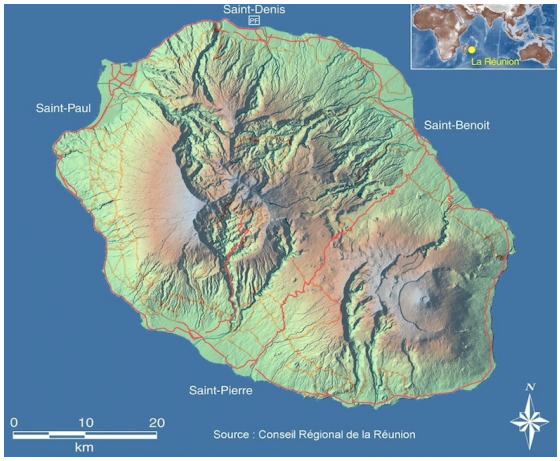


*At the southeast, the highest area represents the volcano called "le Piton de la Fournaise". Source: Conseil regional de la Réunion.*

***Figure 2 Map of La Réunion, France.***

### 4.2. Input data for traffic simulation

The model is applied during the morning peak hour period from 6:00 a.m. to 12:00 a.m., with simulation statistics provided at 20-minutes intervals. The average desired arrival time is set to 8:30 a.m., with a normal distribution of 70 minutes standard deviation. A list of all parameter values, including these, can be found in Table A1 of the appendix.

We first built an Origin-Destination (OD) matrix using data from the INSEE (Daudin, Lieutier, and Besnard, 2014). This data are available for 2011. However, those data are only available at the municipality level. Because METROPOLIS is unable to simulate intra-zone commuting, using the raw data will result in only taking 37.8% of Réunionese commuters into account. In order to increase the number of commuters considered, we also built an OD matrix with a higher resolution using IRIS zones[9] and a probabilistic method. We account for 66.4% of La Réunion's commuters thanks to this transformation. However, due to the tiny sizes of IRIS zones, it is likely that a significant proportion of the remaining commuters will not use a car for commuting. The revised OD matrix has 223 origins and destinations. This OD matrix accounts for 140,121 commuters. The spatial distribution of commuter inflows, or the number of commuters entering the zone, and outflows, or the number of residents leaving it, is shown in Figure 3. The first thing that stands out is the strong correlation between inflows and outflows. Additionally, it is noted that the majority of inflows and outflows are located along the island's coast. We may also see that zones in the South-East of the island nearly never experience inflows or outflows.

9 The National Institute of Statistics' (INSEE) IRIS zone is a French division of the space. They were created to correspond to a population of 2000 indivudals per zone.

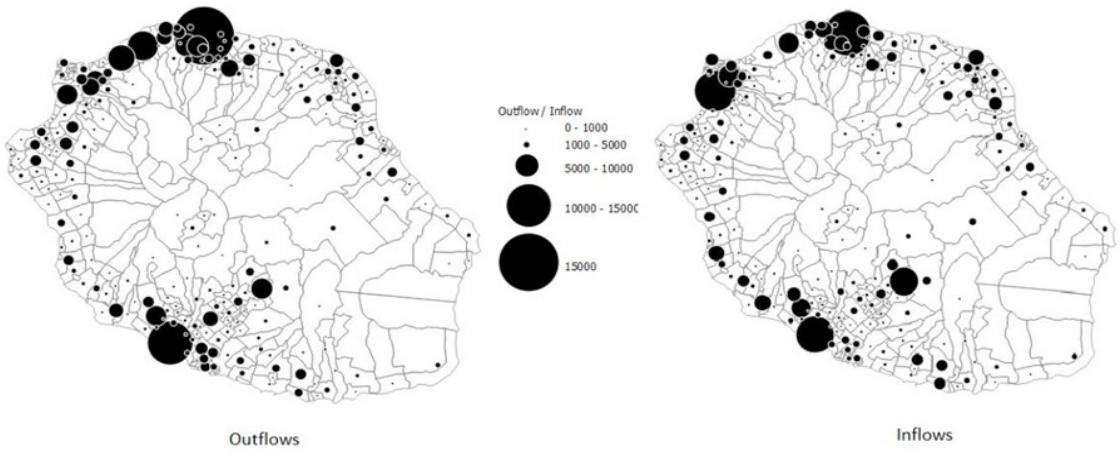


*The left figure shows the number of commuters who leave each zone, while the right one shows the number of commuters who enter each zones.*

***Figure 3 Maps of inflows and outflows of commuters during the morning peak at La Réunion.***

METROPOLIS requires a structured network. Each area, referred to as a zone, is represented by a central point, known as the barycenter of the zone. These points are linked to the rest of the network through connectors, with a maximum of eight connectors (four for entering and four for exiting) connecting each barycenter. Note that the entering and exiting connectors can be asymmetrical. The network consists of 36,340 nodes, which represent intersections and road connections, and 79,824 links, which represent the roadways, with a total length of approximately 11,304 kilometers. In this study, we utilized a simplified OpenStreetMap network that only includes non-residential roadways (as shown in Figure 4). The maximum speed of the network is 130 km/h, with a minimum speed of 10 km/h. The majority of the network has a restricted speed of 50 km/h, which is typical for French urban roads. The network's capacity ranges between 700 and 10,000 vehicles per hour on average. The network is shaped like a ring along the coastline of the island, with only one road crossing it from Southwest to Northeast. This can result in higher congestion and emissions due to longer average travel distances and necessary detours for reaching destinations.

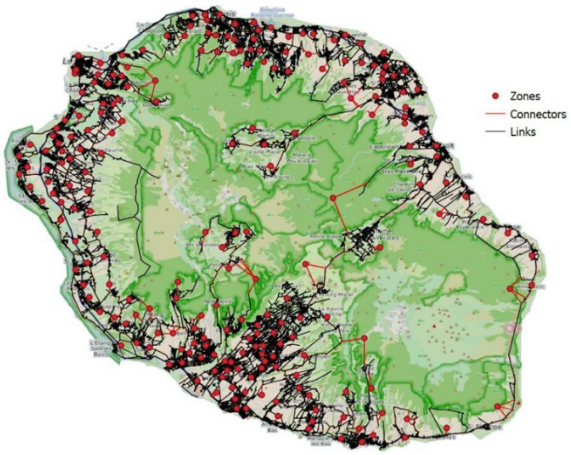


*Sources: OpenStreetMap*

***Figure 4 Road network of La Réunion***

Figure 5 provides the maximum speed of the network is 130 km/h, with a minimum speed of 10 km/h. The majority of the network has a restricted speed of 50 km/h, which is typical for French urban roads. The network's capacity ranges between 700 and 10,000 vehicles per hour on average which refers to the maximum number of vehicles that may drive in a link without causing congestion.

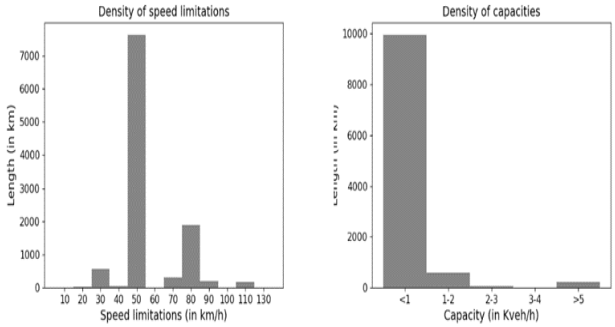


*On the left : Total length of links per speed limit (in km/h), is shown on the left. On the right : total length of links per capacity (in thousands of vehicles per hour). Sources: speed limitations are divided from OpenStreetMap*

***Figure 5 Density distributions of the network***

### 4.3. Input data for emission simulations

Figure 6 describes the French fleet composition. The majority of France's fleet is composed of diesel-powered passenger cars and that the majority of the vehicles comply with EURO 5 and EURO 6 European standard. There is still a significant portion of the fleet that is over 20 years old and falls under EURO 1 and EURO 2, which are known to have higher emissions levels, and should be a priority in the fight against pollution.

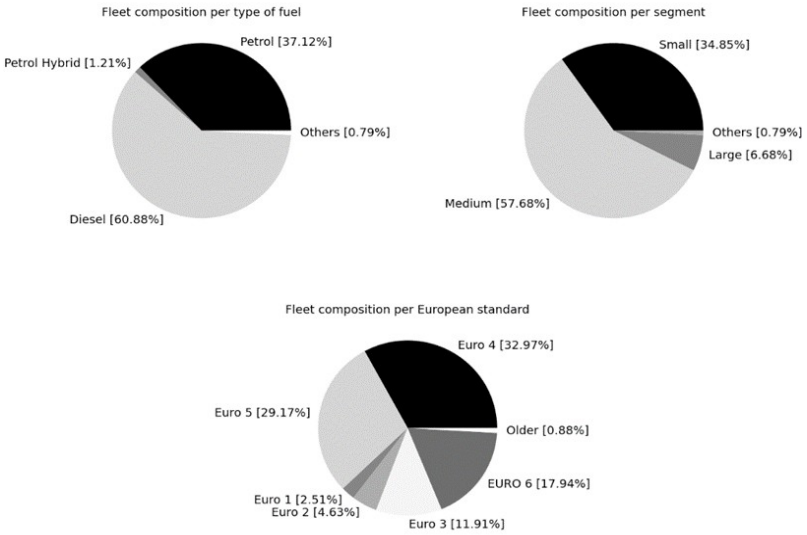


*(a) per motorization types, (b) vehicle size and (c) European norms. Source: Citepa, 2019.*

***Figure 6: French fleet composition***

Figure 7 shows the air pollutant emissions emitted by a mean French passenger car. It is an average emission factor computed considering the national fleet composition (Citepa, 2019), and the emission factors of each type of vehicle of this fleet given by COPERT III database (2019). It is shown that this mean emission factor reachs a minimum emission level at 65 km/h. The emissions from a vehicle's engine tend to follow a U-shaped and asymmetric curve with respect to speed. Indeed, at low speeds, such as in a stop-and-go traffic, the engines need to work harder to get the vehicle moving, which can lead to inefficient fuel combustion and higher emissions of pollutants. Conversely, at high speeds on highways, the engine may not burn more fuel as efficiently, leading to higher emissions of pollutants. Additionally, the increased aerodynamic drag at high speeds can also contribute to higher emissions. In contrast, at medium speeds, the engine runs more efficiently, and the vehicle produces less aerodynamic drag, leading to lower emissions. Specifically, the emissions of CO can vary by a factor of 3.5, while $NO_x$ and $CO_2$ can vary by a factor of 2, and $PM_{2.5}$ can vary by a factor of 1.6. The emissions are computed on each link according to to the mean speed computed by METROPOLIS. They are expected to be higher on low and high-speed links, and the resulting emissions.

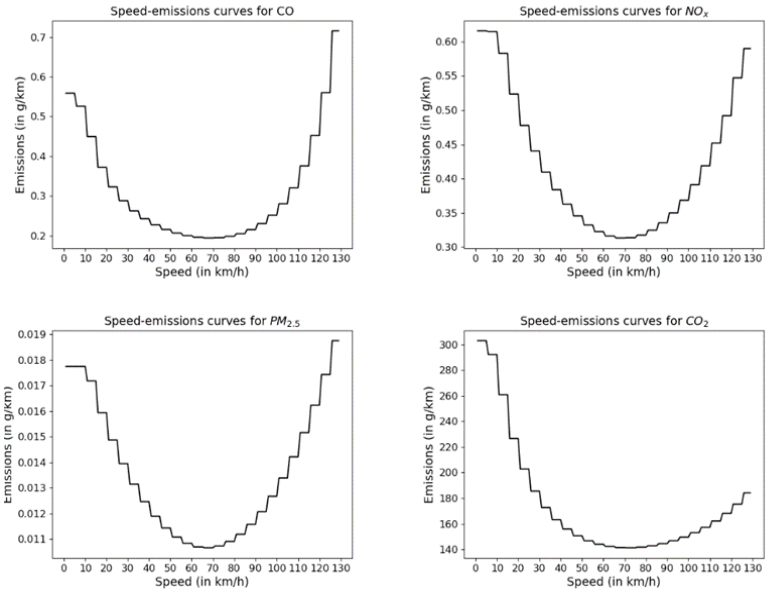


*Computation are made using the national fleet composition (Citepa, 2019) and the emission factors of each type of vehicle of this fleet given by COPERT III database (2019).*

***Figure 7: Mean emission factor (in g/km) of a French passenger car as a function of the speed (in km/h)***

### 4.4. Input data for air pollution concentrations simulations

Air pollution concentrations are computed on a spatial resolution of 100 m. The dispersion module first interpolates the vehicle emissions on a 100 m grid domain. Meteorological data are taken from meteoblue.com. Wind speeds and directions are shown in Figures 8 in terms of wind roses. The predominant direction of the wind at La Réunion is from the North-West to the South-East with an average speed of 7.4 m.s$^{-1}$.

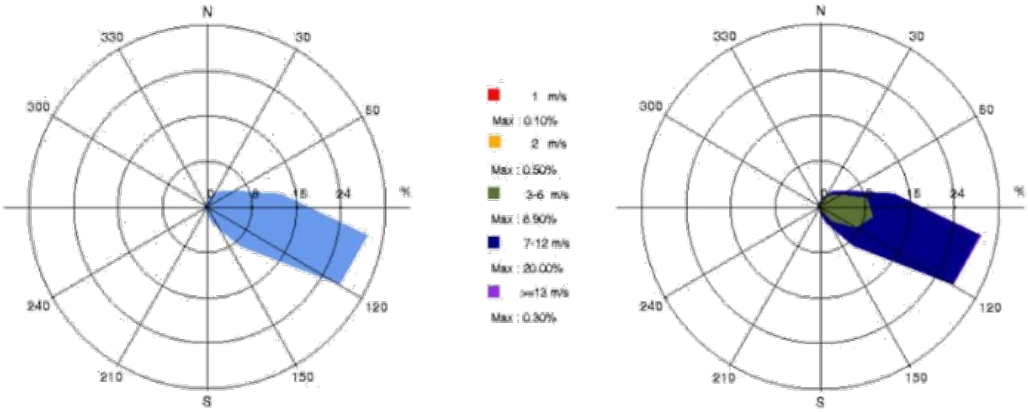


*Source : meteoblue.com.*

***Figure 8: Wind roses observed at the airport of La Réunion's in 2019.***

Figure 9 shows the occurrence of each type of atmospheric stability. It is shown the neutral stability class occurs in over 68% of cases.

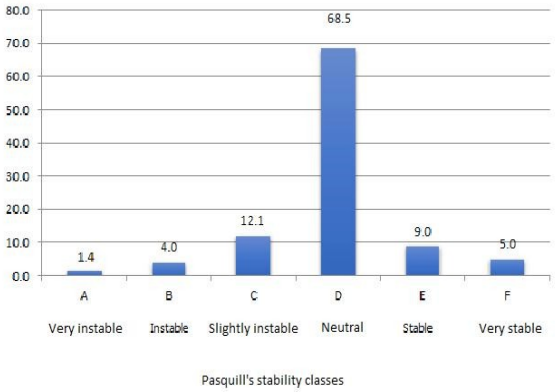


*It is given in terms of frequencies (in percentage of days) per each Pasquill's stabilitity class. Data source : meteoblue.com.*

***Figure 9: Atmopsheric stability observed at the airport of La Réunion in 2019***

### 4.5. **Input data for population exposure simulations**

The French Geographical Institute's (IGN) BDTOPO for 2021 provides information on buildings that described in terms of usages : business operations, services, or industrial are categorised as working places; structures reported for residential purposes are categorised as residential places; few buildings are classified in both previous categories. Buildings localisations are shown in Figure 11 according to their classification. Workplaces are mostly located near the coastline. while residential areas are more dispersed. We notice that the island's southeast and center are largely deserted, respectively, because of the volcano "Le piton de la Fournaise", and few other mountains (see Figure 2).

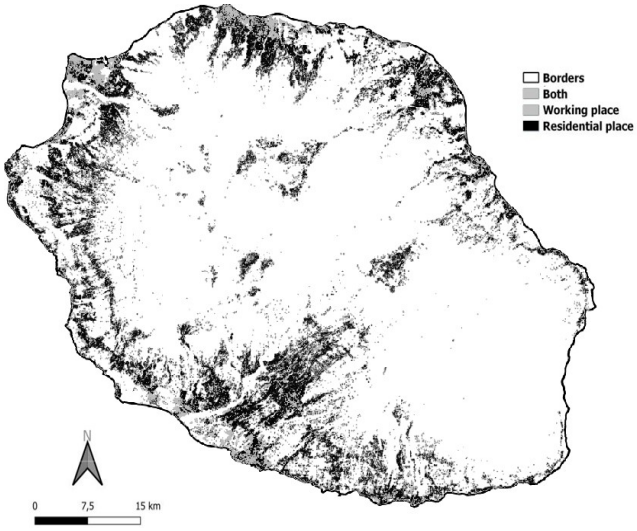


*This map of La Réunion for 2019 shows buildings categorized by their uses as residences, workplaces, or both. Sources: BdTopo (IGN), 2021*

***Figure 11: Location of building according to their classification at La Réunion***

The Landscan population distribution for 2019 (Bhaduri et al., 2002) is depicted throughout space in Figure 10.

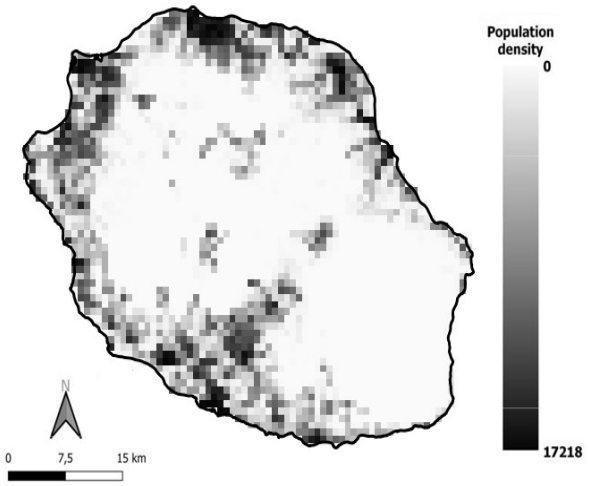


*Sources : Landscan, 2019*

***Figure 10: Spatial population density at La Réunion***

### 4.6. Input data for costs evaluations

Table 3 shows the marginal costs used in this study. Note that CO exposure is significantly lower than that of the others. The marginal costs of exposition for $NO_x$ are by far the highest, followed by those for $PM_{2.5}$. Since $CO_2$ costs are independent of exposure or concentration ($CO_2$ only contributes to global warming and does not have a direct impact on human health), costs are expressed for each ton of $CO_2$ emitted.

***Table 3: Marginal costs of population exposure to several pollutants concentrations***

| Pollutant | Costs | | Authors |
|---|---|---|---|
| $NO_x$ | 0.02634 | $/µg.m$^{-3}$/inh./h | Bigazzi and Figliozzi (2013) |
| CO | 0.00014 | $/µg.m$^{-3}$/inh./h | Bigazzi and Figliozzi (2013) |
| $PM_{2.5}$ | 0.01646 | $/µg.m$^{-3}$/inh./h | Bigazzi and Figliozzi (2013) |
| $CO_2$ | 100 | $/ton | CE Delft (2019) |

*The marginal costs for one person exposed for one hour to one microgram per cubic meter of NOx, CO, and $PM_{2.5}$ are shown in this table in USD. Bigazzi and Figliozzi (2013) used the cost of human life and the probability of death burden to compute these expenses. The costs for $CO_2$ are expressed in USD per ton and are those set forth by CE Delft (2019).*

The overall costs of population exposure to traffic harmful pollutants to health is computing in space and time from the population density and the concentration levels. For areas with high population density and high concentration levels, the overall costs of exposure will likely be higher, while in areas with low population density and low concentration levels, the overall costs will be lower. Therefore, it is crucial to consider both the concentration levels and population density when evaluating the costs of population exposure to pollutants.

## 5. Results: Exposure evaluation of the Réunionese to the traffic air pollution

This section illustrates the outcomes of our chain of models, applied to La Réunion in order to evaluate the population exposure to the traffic air pollution and its costs. The impact of transportation policies will then be assessed.

### 5.1 Traffic simulations

Table 4 provides a summary of the traffic simulations. A 45.7% congestion index suggests that, on average, travel times are about 1.5 times longer than they would be without congestion. With a typical distance of 17.94 kilometers, the average trip lasts 23 minutes and 8 seconds. With an average speed of 50.6 km/h, it can be inferred that most trips take place on urban roads with a speed limit of 50 km/h. Nonetheless, as some residents also travel on national roads with higher speed limit, the average speed is slightly larger than this value.

*Table 4: Summary of METROPOLIS traffic simulations on La Réunion*

| Index name (unity) | Index simulated value | Index observed value | Definition of the index |
|---|---|---|---|
| Peak period duration | 5h 16min | | Simulation duration time starting when 10% of the drivers have reached their destination, and ending when 90% have reached their destination |
| Mean speed (km/h) | 50.6 km/h | | Mean travel speed |
| Trip duration | 23' 8" | 41' 35" – 45'4"** | Mean travel time |
| Trip distance (km) | 17.94 | 25.3* 22.56** | Mean travel distance |
| Congestion Index (%) | 45.7 | 44-60** | Congestion delay as percentage of free-flow travel time on same route |
| Total vehicle (km) | $2.51x10^6$ | $5.1x10^6$* | Total kilometers traveled |

*The outcomes of the METROPOLIS simulation using the baseline parametrization are shown in this table's simulated value column. The observed values from two separate data sources are presented in the Observed Value column. Sources: * Daudin et al. (2014) ** GoogleMaps.*

Figure 12 displays the difference of the vehicle inflows and outflows (the net flow, i.e. the total number of residents entering the network and those leaving it), and the activities per hour on the network (i.e. the road fluxes times the length of the roads, so called the mileage, the number of vehicles kilometers). This activities strongly influence the emissions, as well as the vehicle speed, which is affected by the traffic congestion.

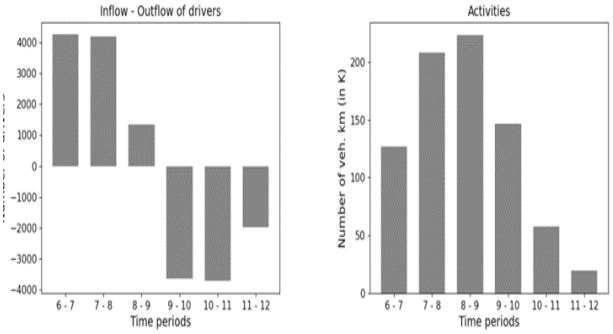


*This figure shows the netflow on the network for each time period, which is the total number of residents entering thenetwork and those leaving it. The total activity, which is provided in thousands of kilometers driven by all residents over a certain time period, is shown in the right graphics. The results of the simulation using the baseline parametrization were used to generate those numbers.*

***Figure 12: Net traffic flows (in vehicles) and activity per hour (in veh.km)***

On those graphs, we can see that the majority of the journey occurred between 7:00 a.m. and 10:00 a.m. Note that the network experiences its highest activity between 7:00 a.m. and 9:00 a.m., with a peak between 8:00 a.m. and 9:00 am. We can see that the largest netflows occurs between 6:00 a.m. and 8:00 a.m., which is consistent with the fact that at the start of the simulation period, few residents are exiting the network while many are entering. The lowest netflows are obtained between 9:00 a.m. and 11:00 a.m.

The weighted congestion percentage, mean travel time, and mean travel distance are computed on daily basis using observations recorded using Google Maps for the 30 most popular trips, with weights allocated proportionally to the number of trips. Computations are carried out for all hours between 6:00 a.m. and 12:00 p.m.. To account for the presence of two peaks in a day, the reported values of total vehicule kilometers has to be multiplied by a factor of 2, and it is noteworthy that the resulting values are remarkably similar. Since the majority of trips occur during peak hours of 7:00 a.m. to 9:00 a.m., additional calculations are made solely for those hours, yielding higher values. Table 4 shows that the simulated value of the congestion index matches its lower bound as established by Google Maps. However, the mean travel distance and time is overestimated.

### 5.2 Emission simulations

METROPOLIS traffic simulations (activities and mean speed on each link) coupled with EMISENS model allows to compute the traffic air pollutant emissions. These emissions are described in Table 5.

***Table 5: Total air pollutant emissions computed over La Réunion***

| **Morning peak (6:00 a.m. - 12:00 p.m.)** | | | | |
|---|---|---|---|---|
| **Pollutants** | **Total (kg)** | **Per driver (g)** | **Per inhabitant (g)** | **Per km (g)** |
| $NO_x$ | 973 | 6.95 | 1.13 | 0.39 |
| CO | 732 | 5.23 | 0.85 | 0.29 |
| $PM_{2.5}$ | 187 | 1.34 | 0.22 | 0.07 |
| $CO_2$ | 393811 | 2812 | 458 | 157 |
| **Per year (All days)** | | | | |
| **Pollutants** | **Total (T)** | **Per driver (kg)** | **Per inhabitant (kg)** | |
| $NO_x$ | 710.8 | 5.1 | 0.83 | |
| CO | 534.5 | 3.8 | 0.62 | |
| $PM_{2.5}$ | 136.6 | 1 | 0.16 | |
| $CO_2$ | 287482 | 2053 | 334 | |

*This table shows the amount of each sort of pollution that was released annually and during the morning peak, which is the time frame from 6 a.m. to 12 p.m. Estimates for each year are created by multiplying the morning peak results by 2x365. The parametrization of the baseline is used to estimate those values. Total is the total amount of emissions for each category of pollutant. Total emissions are divided by the number of drivers in our baseline parametrization to get emissions per driver. The total emissions are divided by the population of Réunion to get the emissions per inhabitant. The total emissions are divided by the amount of kilometers that are traveled in our baseline parametrization.*

We can observe that each driver emits around 2 tons of $CO_2$ annually which is in line with the value of 2.46 tones estimated by the Observatoire Energie Réunion (2020)[10] for the whole transportation sector (including air and maritime transport). Each driver also emits 5.1 kg of $NO_x$ per year, which is slightly lower than the estimate of 8 kg/driver/year for Strasbourg made by Ho et al. (2014). The discrepancy between those two numbers was explained by the great evolution of the vehicle fleet between those two studies (less diesel cars). Finally, we can see that each driver annually releases 3.8 kg of CO and 1 kg of $PM_{2.5}$.

Figure 13 displays the total amount of air pollutants released over the course of each hour. We can see that the four curves exhibit the exact same profile as the activity profile. This shows that the results of the emission model were not influenced by the significant congestion seen in the METROPOLIS results. Additionally, We note that the scales between each pollutant for each time period are consistent with those shown in Table 3.

10

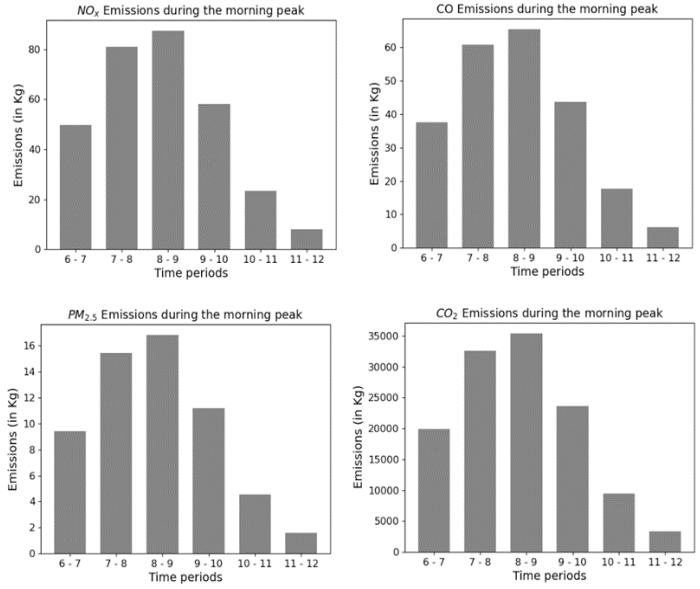


*These charts display the quantity of each type of pollution that was released during the morning peak, which is from 6:00 a.m. to 12 p.m. These values are estimated using the baseline parametrization.*

***Figure 13: Total traffic air pollutant emissions per hour during the morning peak***

Since fleet composition, congestion, and other network factors have a significant impact on the emissions of different pollutants, it is important to note that these results are quite challenging to compare with other statistics in the literature.

### 5.3 Air pollution simulations

In order to evaluate the performances of our chain of models, we compared hourly observed $PM_{2.5}$ from Atmo Réunion for the year 2019 between 6:00 a.m. and 12:00 a.m. with data estimated using our framework with the baseline parametrization. These data are available for four different air pollution control stations. Because our chain can only estimate pollutant emissions and concentrations attributable to road traffic, we must first identify stations that are affected by pollution connected to road traffic. To do this, we analysed the average hourly concentrations of NO, $NO_2$, and $PM_{2.5}$, three pollutants highly emitted by road transport. Map of the different air control stations and graphics are available in Appendix A3. These graphics show that just two stations appear to be clearly impacted by road traffic (stations “Route des Tamarins” and “Joinville”), with hourly concentration profiles showing two picks, one during the typical morning commute and the other one during the evening commute. To allow a comparison, an average daily observed concentration is first computed for hours where road traffic is assumed to be minimal, which are typically before 3 a.m., between 12 p.m. and 4 p.m, and after 10 p.m.. This average is then subtracted from the hourly daily average of concentrations measured during the simulation period (6 a.m. to 12 p.m.) in order to estimate the observed maximum time variations of the traffic contribution.

Figure 14 shows the comparisons of this computed maximum hourly traffic contribution with the simulations.

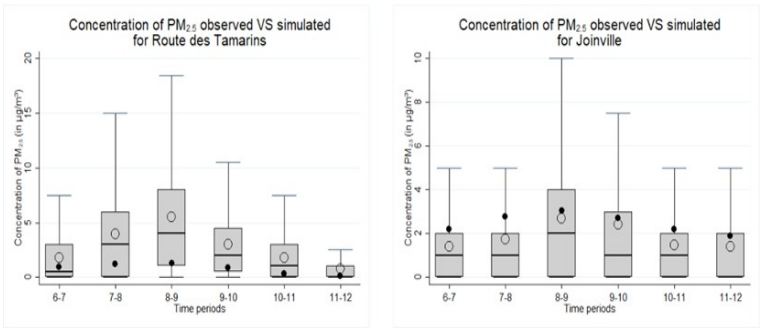


*The $PM_{2.5}$ observed concentrations at the air pollution station Route des Tamarins during the morning peak, which is the time period from 6 a.m. to 12 p.m., are shown using boxplots in the left figure. Our predicted concentrations at the station's location are represented by the black dots. For our baseline parametrization, they are computed using our Gaussian plume model, in which we integrated the outcomes of our emissions model. The identical outcomes are shown in the right figure, but for the Joinville air pollution station. Source: AtmoRéunion, 2019*

***Figure 14: Observed versus simulated concentration of $PM_{2.5}$ during the morning peak at La Réunion.***

The hourly simulated concentrations are underestimated or overestimated the hourly average traffic contribution, depending on the location of the station. While our simulated concentrations always keep between the second and third quarters of the distribution of hourly traffic contribution, the model is not able to fully represent the hourly variation of the daily maximum traffic contributions as observed (globally here seen as underestimated). This is especially noticed on Joinville station (the simulated concentrations are estimated into the first quarter of the distribution of the traffic contributions before 3 a.m., between to 12 a.m. and 4 p.m., and after 9 p.m.). One can note that constant and uniform wind speed and directions are considered in the present version of the model, neglecting their hourly variations and their impact on the local dispersion of the air pollution (the effect of buildings on the wind speed and the directions, very complex to simulate, is not considered).

### 5.4 Exposure evaluations

Table 6 describes the population costs exposure to air pollution. Note that $NO_x$ is the pollution with the highest marginal population exposure costs, largely costlier than the CO2 and PM2.5 air pollution. Population exposure to pollutant concentration is low in La Réunion due to the geographical correlation between road distribution and population, which may account for the significant discrepancies between our findings and those reported in the literature.

***Table 6: Descriptive statistics for population costs exposure***

| **Morning peak (6:00 a.m. - 12:00 p.m.)** | | | | |
|---|---|---|---|---|
| **Pollutants** | **Total ($)** | **Per driver ($)** | **Per inhabitant ($)** | **Per km ($)** |
| $NO_x$ | 71696 | 0.5119 | 0.0834 | 0.0286 |
| CO | 139 | 0.001 | 0.0002 | 0.0001 |
| $PM_{2.5}$ | 8589 | 0.0613 | 0.01 | 0.0034 |
| $CO_2$ | 38175 | 0.2726 | 0.0444 | 0.0152 |
| All | 118599 | 0.8468 | 0.1379 | 0.0473 |
| **Per year (All days)** | | | | |
| **Pollutants** | **Total (k$)** | **Per driver ($)** | **Per inhabitants ($)** | |
| $NO_x$ | 52338 | 373.7 | 60.9 | |
| CO | 101 | 0.7 | 0.01 | |
| $PM_{2.5}$ | 6269 | 44.7 | 7.3 | |
| $CO_2$ | 27867 | 199 | 32.4 | |
| All | 86577 | 617.5 | 100.7 | |

*The morning peak and annual expenditures for each type of pollution are displayed in this table. The morning peak is the period from 6 a.m. to 12 p.m. The morning peak values are multiplied by 2x365 to obtain estimates for each year. These values are computed using the outputs of our population movement module combined with the outputs of our dispersion model. These values are estimated using the baseline parametrization. Total is the sum of the costs for each type of pollution. In our baseline parametrization, all costs are divided by the number of drivers to obtain costs per driver. The costs per inhabitant are determined by dividing the total costs by the population of La Réunion. The costs per kilometers are obtained by dividing the total costs by the number of kilometers driven in our baseline parametrization.*

Figure 15 shows the costs of exposure to pollutants as a function of time. We note that the time profiles mirror those of activity and pollution, but not for the initial time period. The costs of exposure to $NO_x$, CO, and $PM_{2.5}$ estimated between 6 a.m. and 7 a.m. is large. This may be accounted for by the fact that individuals start their trips from their homes. Therefore, population exposure and its related costs at the beginning of the simulation are higher. Similar to the descriptive table, we can rank pollutants for each time period in the same order from least to most expensive.

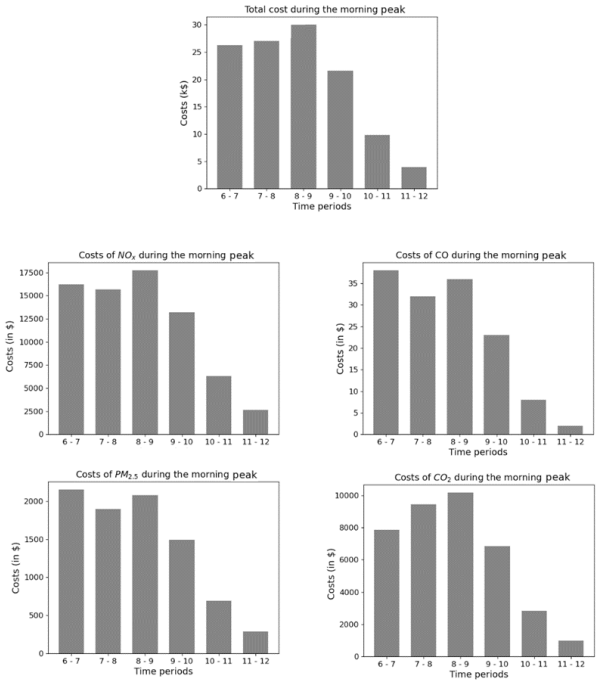


*These charts display the costs of each type of pollution during the morning peak, which is from 6:00 a.m. to 12 p.m. These values are computed using the outputs of our population movement module combined with the outputs of our dispersion model. These values are estimated using the baseline parametrization.*

***Figure 15: Pollutants exposition costs per time period***

According to CE Delft (2020), the yearly cost of population exposure to $PM_{10}$, $PM_{2.5}$, $NO_2$, and $O_3$ in London and Paris is $1294 and $1602 per inhabitants, respectively. Note that our results are also quite low compared to those of Vlachokostas et al. (2012) and Martinez et al. (2018) which find respectively values of $4500 and $3601. However, these costs take in account cost of population exposure to pollutant from all sources. Since we find with our chain of models on La Réunion that this cost is about $100.7.

Several explanations of this low value could be discussed. First La Réunion is an island and that there is no transit traffic, which makes up around 50% of all traffic in Paris. In addition, our model is unable to model non-working travels, intra-commuting, and estimate the exposure and related costs experienced during the commuting process. This will therefore raise the overall cost of population exposure to traffic pollution in our model.

Notably, population exposure is not expressly taken into account in the majority of the studies. Our study take into account the spatial and temporal distribution of both population and concentrations. While in CE Delft (2020) for example, all residents are assumed to be exposed to the average concentrations observed in the studied area. Therefore, this could made a significant differences.

However, more vehicles will create more pollution, but this might be due to two separate channels, the first being mechanical. The second is more tricky; more traffic will always result in increased congestion, but congestion may have a positive or negative effect on the levels of pollutants released. Finally, take notice that road traffic connected to public transportation is not taken into consideration by our models. Additionally, while population exposure is primarily determined by the distribution of population and roads across space, differences in fleet composition, traffic flows, and congestion have a significant impact on pollutant emissions. It is so challenging to compare population exposure to vehicle traffic pollution statistics across various nations, regions, or municipalities.

## 6. Results: Exposure evaluation of the Réunionese to the traffic air pollution

The fleet composition and congestion in La Réunion were the main contributors to road traffic pollution, according to the prior sections. In order to assess proposed laws and give input on their efficacy, we test fleet composition restrictions in this area. In order to evaluate its performances, we also examine a policy that reduced congestion.

### 6.1 Renewal of the oldest cars by electric vehicles

"What effect would replacing thermal automobiles with EVs have?" is what this scenario explores. Since many people and authorities today wish to replace thermal vehicles with electric ones, this appraisal seems to be quite essential. Following a vote in the European Union in June 2022, the sale of new thermal vehicles will cease in 2035. Therefore, understanding how such measures could affect the well-being of populations is essential.

We built five different scenarios which relies on European passenger cars standards (EURO I to EURO VI). Those standards has been putted in place by the European Union to ensure that all passenger cars meet a minimum level of safety, environmental protection, and energy efficiency.

The least restrictive option is EURO II, where EVs are only used to replace the oldest, EURO I and EURO II passenger cars. The All scenario is the most limiting one. In this scenario, we outlaw all thermal vehicles and substitute EVs. In all other scenarios, EURO III, EURO IV, and EURO V, the goal is to prohibit any passenger automobiles with standards that are older than the corresponding versions of these standards. Figure 16 demonstrates that, in the All scenario, emissions are reduced to zero, with the exception of $PM_{2.5}$, which only experiences a 20% reduction. This may be accounted for by the fact that our model estimates $PM_{2.5}$ non-exhaust emissions, which are unaffected by motorization. Since the fleet mix includes varying numbers of each standard vehicle, this figure alone might be challenging to analyze. It is important to keep in mind that only 8% of the fleet is older than EURO II, compared to 20%, 53%, and 82% for EURO III, EURO IV, and EURO V, respectively.

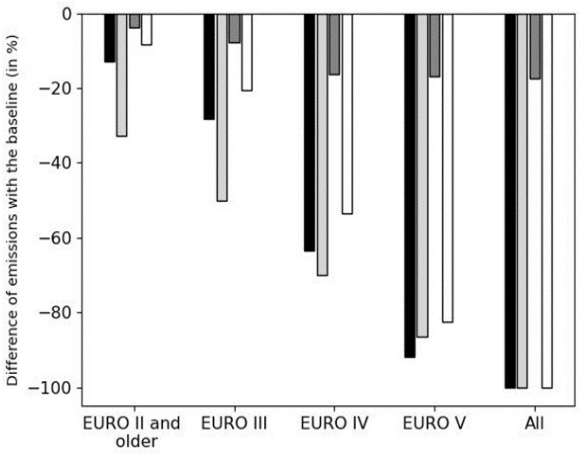


Black: $NO_x$; Light Grey : CO; Dark Grey: $PM_{2.5}$; White: $CO_2$

*This graph shows the differences in emissions for each type of pollutant between the emissions from our five scenarios and the emissions from baseline parametrization. A scenario where all thermal vehicles with a European norm of EURO II or older are replaced by electric vehicles is referred to as "EURO II and older." Thermal cars that met an older or equivalent standard to EURO III were replaced with those that did. The reasoning behind EURO IV and EURO V is the same for each European standard. The All scenario calls for the replacement of all thermal vehicles with electric ones.*

***Figure 16: Comparison of emissions at La Réunion between the baseline and the different scenarios based on European standard***

Elasticity refers to the degree to which the quantity of pollutants change in response to fleet composition changes. The elasticities of pollutant emission in response to a replacement of 1% of thermal cars are shown in Table 7 for each European standard.

***Table 7: Elasticities of pollutant emissions with respect to European standard for La Réunion***

| European Standard | $NO_x$ | CO | $PM_{2.5}$ | $CO_2$ |
|---|---|---|---|---|
| **EURO II** | 1.6 | 4.1 | 0.46 | 1.04 |
| **EURO III** | 1.29 | 1.02 | 0.34 | 1.02 |
| **EURO IV** | 1.06 | 0.6 | 0.26 | 1 |
| **EURO V** | 0.99 | 0.57 | 0.02 | 1 |
| **EURO VI** | 0.44 | 0.75 | 0.02 | 0.98 |

*The elasticities of pollutant emission in response to a one percentage point reduction in thermal cars by European regulations are shown in this table. These figures were estimated using the outcomes of our five scenarios, in which we sequentially outlawed thermal vehicles in accordance with their European standard and compared the resulting emission to that determined by our baseline parametrization.*

We see that, unlawful thermal vehicles that meet the EURO II or older criteria always result in a greater reduction of pollutant release. This is consistent with the fact that older vehicles are subject to fewer strict emissions regulations. As a result, this might also be used to explain why emissions are becoming less elastic according to the European standard. With CO as an exception, which displays greater elasticity for the EURO VI standard. The composition of the EURO VI fleet may be to blame for this. Diesel EURO VI vehicles are subject to stronger CO rules than gasoline vehicles. Therefore, CO emissions for this standard are greater for the EURO IV fleet if there is a higher proportion of petrol vehicles than in other fleets, which results in a higher elasticity. Therefore, a finer decompositon of the fleet needs to be done in order to better assess the impact of prohibiting thermal cars. We should estimate elasticity for each vehicle depending on its type, motorization, and standard. Using those elasticities it is possible to quantify in term of pollutant release quantity the effect of those policies. Knowing that 1% of the fleet consists of 1,400 vehicles and that 1% of the annual emissions consists of 7,108 kg of $NO_x$, 5,345 kg of CO, 1,336 kg of $PM_{2.5}$, and 2,874,821 kg of $CO_2$. As a result, those effects may be measured. For example, we can show that replacing one EURO III thermal car will reduce the amount of $NO_x$, CO, $PM_{2.5}$, and $CO_2$ emissions per year by 8.1 kg, 15.7 kg, 0.44 kg, and 2135.6 kg, respectively.

***Table 8: Elasticities of costs with respect to European standard for La Réunion***

| European Standard | $NO_x$ | CO | $PM_{2.5}$ | $CO_2$ |
|---|---|---|---|---|
| **EURO II** | 1.54 | 7.29 | 0.44 | 1.04 |
| **EURO III** | 1.29 | 1.56 | 0.3 | 1.02 |
| **EURO IV** | 1.08 | 0.46 | 0.26 | 1 |
| **EURO V** | 1.01 | 0.27 | 0.03 | 1 |
| **EURO VI** | 0.42 | 0 | 0.02 | 0.98 |

*The elasticities of total costs in response to a one percentage point reduction in thermal cars by European regulations are shown in this table. These figures were estimated using the outcomes of our five scenarios, in which we sequentially outlawed thermal vehicles in accordance with their European standard and compared the resulting costs to that determined by our baseline parametrization.*

For each European standard, Table 8 displays the elasticities of population costs exposure in response to a replacement of 1% of thermal automobiles. When costs are taken into account instead of emissions, we see that this time, prohibiting older or EURO II passenger cars always results in the biggest cost savings. Since the cost of $CO_2$ does not rely on population exposure, which is why elasticities with respect to emission or to population exposure for $CO_2$ exhibit the same values. However, this allows us to emphasize how critical it is to consider population distribution through time and place in order to accurately estimate the cost of population exposure.

Additionally, we should be aware that the elasticities for $PM_{2.5}$ and $NO_x$ with regard to pollutant emissions and population cost are relatively similar. Finally, we see that elasticities are fast falling for CO. We should be conscious that for EURO IV, this elasticity essentially vanishes. As before, we also compute the population exposure costs savings associated with switching from one type of vehicle to an EV. Remember that 1,400 vehicles make up 1% of the fleet. Knowing that 1% of the population's annual exposure costs equals \$523,380 for $NO_x$, \$1,010 for CO, \$62,690 for $PM_{2.5}$, and \$278,670 for $CO_2$. For instance, we determine how much money would be saved each year if one EURO III thermal automobile was replaced with an EV. It turns out that these savings are, \$482.26 for $NO_x$, \$1.1 for CO, \$13.43 for $PM_{2.5}$, and \$203.03 for $CO_2$ which results in a total yearly saving of \$699.82.

We have demonstrated that switching from thermal to EVs will reduce both the population's exposure to road traffic pollution and pollutants emissions. Additionally, switching all thermal vehicles to electric ones will completely eliminate all $NO_x$, CO, and $CO_2$ emissions as well as the exposure costs linked to them. This conclusion does not apply to $PM_{2.5}$, as a significant portion of it is created by road abrasion, brake wear, and tyre wear rather than by the engine. Additionally, this effect varies greatly amongst European standards. The greatest reduction in pollution emission and population exposure costs will result from the outlawing of older automobiles.

It is important to highlight that our integrated chain of models only in-cluded costs related to vehicle motion. Because both the production of power and the manufacture and recycling of batteries are famously bad for the en-vironment, we do not take any of this pollution into account. Zheng et al. (2020) when comparing the difference in pollution emissions between thermal and EVs for China, considering the entire lifecycle of the vehicle, as well as the pollution released during the generation of power. They found that the average gasoline automobile emits 35% more greenhouse gases than an EV. While $PM_{2.5}$ emissions are unaltered, $NO_x$ emissions are reduced by 34%. As a result, our findings must be considered to be an upper limit on the amount that could be saved in population costs exposure, and emissions. A Réunionese EV is predicted to generate 129.4 $gCO_2/km$[11]. It is therefore possible to compute the well-to-wheels emissions for each scenario using our findings. Table 9 enables us to moderate the results shown above. We should note that considering well-to-wheels emissions of EVs will result in the scenario where we ban all thermal vehicles to only reduce $CO_2$ emissions by about 44% against 100% while take only emitted pollutants into account. Therefore, to account for this effect, the elasticities of both emission and population exposure costs for $CO_2$ should be divided by two.

***Table 9: Emissions of $CO_2$ while considering well-to-wheels emissions of electric vehicles***

| Scenario | Electric vehicle (T) | Thermal vehicles (T) | Total Emissions (T) | Difference (%) |
|---|---|---|---|---|
| **EURO II** | 26 | 361 | 387 | -1.7 |
| **EURO III** | 64.7 | 313.1 | 377.8 | -4.1 |
| **EURO IV** | 171.8 | 183.2 | 355 | -9.9 |
| **EURO V** | 266.6 | 69.4 | 336 | -14.7 |
| **All** | 324.8 | 0 | 324.8 | -17.5 |

*The amount of $CO_2$ emitted by electric vehicles in each scenario is shown in the electric vehicle columns of the table. These numbers were computed using a value of 129.4g $CO_2$/km. The total $CO_2$ emissions from our 5 scenarios are shown in the thermal vehicles columns. The $CO_2$ emissions from both thermal and electric vehicles are added to determine total emissions. The difference column shows the variation in emissions between the total emissions columns for each scenario and the baseline parametrization $CO_2$ emissions.*

Our study of strategies to switch from thermal to EVs demonstrates that banning older vehicles results in greater reductions in pollutant emissions. According to our study, $NO_x$ and CO emissions could be fully eradicated if all thermal vehicles were switched out for electric ones. Nevertheless, $PM_{2.5}$ emissions are only reduced by 20%. However, when the energy production process is taken into account, EVs only lower $CO_2$ emissions by about 17.5%. The results of our study, including the elasticity of population exposure costs and emissions in response to a replacement of thermal cars with EVs, are valuable for extrapolating future benefits of such policies. This information can help decision-makers determine the most effective strategies for reducing emissions and promoting a cleaner, more sustainable transportation system.

### 6.2 Flexibility in working hours

In this scenario, we test the following hypothesis: "What influence would giving employees more control over their working hours have?". We change the desired arrival time distribution standard deviation from 1 h 10 min to 1 h 30 min in order to analyse this policy. This policy permits employees to arrive at work sooner or later. Table 10 displays the outcomes of our dynamic traffic model when residents are given more flexible work schedule options. The duration of the peak period has slightly increased (1%). Additionally, we see that the network's average speed is significantly higher than the one produced using the baseline parametrization (50.6 km/h), at 54.82 km/h. As a result, the mean travel time is decreased by 8% as a result of this notable increase in average speed. Those outcomes are mostly the result of a significant decrease in the congestion index (from 45.7% to 34.7%). Finally, note that this legislation has essentially no impact on mean trip distance and total vehicle kilometers.

11 The above data is based on two pieces of information: first, the Observatoire Energie Réunion (2020) reports a number of $719gCO2.kWh^{-1}$ for 2019; second, Holdway et al. (2010) report that a French car consumes 0.18 $kWh.km^{-1}$ of energy.

***Table 10: Descriptive statistics of METROPOLIS simulation while adding flexibility in working hours***

| Statistic | Simulated value | Difference (%) |
|---|---|---|
| Peak period duration | 5 h 19 min | 1 |
| Speed | 54.82 km/h | 8.3 |
| Trip duration | 21 min 16 sec | -8 |
| Trip distance | 17.83 km | -0.6 |
| Congestion Index | 34.66% | -24.2 |
| Total vehicle km | $2.5x10^6$ | -0.3 |

*The outputs of the METROPOLIS simulation adopting the flexible hours scenario parametrization are shown in this table in the simulated value column. The difference column displays the percentage difference between results obtained using the baseline parametrization and those obtained using the flexible hour scenarios.*

Table 11 displays the EMISENS findings for our novel situations in which flexible work schedules are permitted. We might start off by noting that this policy decreased the total amount of pollutants that were emitted. Similar decreases are seen for $NO_x$ and CO, at 1.7%. With a reduction of roughly 2.4%, $PM_{2.5}$ is obviously more impacted by this legislation than other pollutants.

***Table 11: Descriptive statistics of pollutants emissions while adding flexibility in working hours***

| Pollutants | Total (T) | Per driver (kg) | Per inhabitants (kg) | Difference (%) |
|---|---|---|---|---|
| **$NO_x$** | 698.4 | 4.99 | 0.812 | -1.7 |
| **CO** | 525.7 | 3.75 | 0.611 | -1.7 |
| **$PM_{2.5}$** | 133.3 | 0.95 | 0.155 | -2.4 |
| **$CO_2$** | 281695.1 | 2011.2 | 327.5 | -2 |

*This table displays emissions for each types of pollutants. They have been produced using the flexible hour scenario parametrization. Total is the total amount of emissions for each category of pollutant. Total emissions are divided by the number of drivers in our flexible hour parametrization to get emissions per driver. The total emissions are divided by the population of Réunion to get the emissions per inhabitant. The total emissions are divided by the amount of kilometers that are traveled in our flexible parametrization. The emissions differences between the outcomes achieved using the flexible hour parametrization and those acquired using the baseline parametrization is indicated by the difference columns.*

The population costs exposure related to our flexible work schedules scenario is shown in Table 12. When considering population costs exposure, we may see that conclusions drawn from emissions results do not hold. We should be aware that the population costs exposure for $NO_x$, $PM_{2.5}$, CO and are larger than those determined by baseline parametrization. First, these results can be explained by the fact that more individuals would choose alternate routes because traffic on a specific link is less congested than it was in the baseline scenario, raising emissions in locations with higher population densities. The second rationale is that lessening congestion will lead to faster speeds, and because the emission curves are convex, this could lead to higher or lower emissions depending on the initial speed. Therefore, if emissions are significantly increased in less populated areas and lowered in more crowded areas. The overall emissions level may drop as a result, but the cost of population exposure may rise. As for emissions, we should note that $CO_2$ costs fall by 2%, which is consistent with the fact that $CO_2$ costs do not account for population exposure. The significance of considering both population and concentration distribution for estimating the cost of population exposure to road traffic pollution is once again highlighted by these results.

*Table 12: Descriptive statistics of costs while adding flexibility in working hours*

| Pollutants | Total (k$) | Per driver ($) | Per inhabitant ($) | Difference (%) |
|---|---|---|---|---|
| **$NO_x$** | 57213 | 408.5 | 66.5 | +9.3 |
| **CO** | 107 | 0.8 | 0.1 | +5.9 |
| **$PM_{2.5}$** | 6430 | 45.9 | 7.5 | +2.6 |
| **$CO_2$** | 27310 | 195 | 31.8 | -2 |
| **All** | 91061 | 650.2 | 105.9 | +5.2 |

*This table displays costs for each types of pollutants. They have been produced using the flexible hour scenario parametrization. Total is the total cost for each category of pollutant. Total costs are divided by the number of drivers in our flexible hour parametrization to get costs per driver. The total costs are divided by the population of Réunion to get the costs per inhabitant. The total costs are divided by the amount of kilometers that are traveled in our flexible parametrization. The costs differences between the outcomes achieved using the flexible hour parametrization and those acquired using the baseline parametrization is indicated by the difference columns.*

Our analysis emphasizes the critical importance of considering population exposure in both time and location when assessing program effectiveness. Granting employees greater control over their work schedules may reduce congestion, but it may also increase population exposure costs for pollutants such as $NO_x$, CO, and $PM_{2.5}$, while lowering $CO_2$ emissions levels. Thus, it is important to note that policies that aim to reduce pollutant emissions may lead to increased population exposure costs, which highlights the need for policymakers to carefully weigh the potential trade-off between emission reduction and population exposure increase when evaluating policy options.

One reason for this trade-off could be the spatial distribution of emissions, where the policy may reduce emissions in areas with lower population density but may increase emissions in areas with higher population density. This could be due to higher transportation demand in areas with more people. Thus, if the policy does not address those specific areas, it may not achieve the desired reduction in pollution levels across the entire population. As a result, some individuals may experience a reduction in their exposure to pollutants, while others may experience an increase.

Another reason is the temporal distribution of traffic. The policy leads to a more dispersed distribution of traffic throughout the day, with fewer vehicles on the road during some hours. However, this may also lead to more prolonged periods of higher pollutant concentrations, resulting in higher average pollutant concentrations. As a result, the policy may lead to lower emissions during specific times of the day, but it may also lead to higher population exposure costs.

Therefore, policymakers need to carefully weigh the trade-off between reducing emissions and increasing population exposure when evaluating policy options. It is essential to take a comprehensive approach that addresses both emission reduction and population exposure reduction goals. This could involve implementing measures to promote cleaner transportation options, enhancing air quality monitoring systems, and educating the public about the health impacts of air pollution. By adopting a comprehensive approach, policymakers can ensure that their policies have the greatest overall benefit for public health and the environment.

## 7. Conclusions

In this paper, we developed an integrated chain of models (METRO-TRACE) to assess which fraction of the population is exposed to air pollution from roads. We integrate a dynamic traffic simulation model, an emission model, a dispersion model, and a population exposure model. In our model, time-discrete speed and flow distributions are coupled with extremely high-resolution population density data. We estimate the cost of exposing people to pollutants like nitrogen oxides ($NO_x$), carbon monoxide (CO), and particulate matter with diameter lower than 2.5 μm ($PM_{2.5}$) with the help of this novel methodology. We also consider the cost of carbon dioxide ($CO_2$).

We computed the pollution-related costs in La Réunion, France, using our METRO-TRACE model. According to our estimate, the pollution cost of La Réunion is rather low at $100.7 per year per person. However, this figure solely accounts for primary pollutants, and only considers working commutes between zones. As a result, our predictions do not include all pollution contributions.

We also examined the potential effects of banning thermal vehicles and replacing them with electric ones. Our findings indicate that the reduction in population exposure to road pollution is greater for older vehicles. We estimate that prohibiting thermal vehicles would completely eliminate $NO_x$, CO, and $CO_2$ emissions, but only about 17% of $PM_{2.5}$ emissions. Further research is needed to investigate the heterogeneous impact of outlawing thermal vehicles in terms of

their fuel type, category, and specifications. Additionally, note that the reduction in $CO_2$ emissions when taking into account ones resulting from the electricity production process is only around 17.5%, highlighting the need for significant efforts to efficiently supply electricity for electric vehicles (EVs) in La Réunion.

According to our research, giving workers more flexibility with their work hours can reduce network-wide congestion, resulting in higher speeds and shorter travel times. Moreover, all pollutants' emission levels drop as a result of this. Notwithstanding this, our simulation revealed a divergent trend between population exposure costs and emissions, with costs for CO, $PM_{2.5}$, and $NO_x$ rising and those for $CO_2$ falling. These findings demonstrate the complexity of the transportation system's effects on its associated costs of population exposure. These conclusions on the effect of employee work schedules on transportation would not have been feasible without METRO-TRACE. More investigation is required to better comprehend these systems.

This chain might be improved to estimate and take into account population exposure to pollution while they are travelling, which should mechanically increase the population exposure cost. Moreover, our dispersion model consider static parameters across time and space. Therefore, more effort to increase the heterogeneity level of this model could be highly beneficial. Additionally, we neglected to consider truck traffic, and public transportation in our analysis. However, there is still much work to be done on our chain of models to make it simple to utilize for future research and to test different scenarios. Nevertheless, La Réunion is a rather small area, therefore it could be worthwhile to test our chain's computing performance on a larger, more extended territory such as Île-de-France.

In conclusion, our study has shown that there are several strategies to reduce the population’s exposure to road traffic pollution. This could be achieved through implementing policy-based laws as well as societal changes. Nonetheless, it is crucial to evaluate the various situations before putting them into action because doing so could sometimes lead to harmful consequences.

**Competing interests**

The authors have no relevant financial or non-financial interests to disclose.

## References


- Arnott, R., de Palma A., & Lindsey, R. (1993). A Structural Model of Peak-Period Congestion: A Traffic Bottleneck with Elastic Demand., The American Economic Review 83, no.1: 161–79. https://www.jstor.org/stable/2117502
- Akbar, P., & Duranton, G. (2017). Measuring the Cost of Congestion in Highly Congested City: Bogotá. CAF – Working paper; N° 2017/04, Buenos Aires: CAF.
- Almetwally, A., A., Bin-Jumah, M., & Allam, A., A. (2020). Ambient air pollution and its influence on human health and welfare: an overview. Environ Sci Pollut Res 27, 24815–24830 https://doi.org/10.1007/s11356-020-09042-2
- Badyda, A.J., Grellier, J., & Dąbrowiecki, P. (2016). Ambient PM2.5 Exposure and Mortality Due to Lung Cancer and Cardiopulmonary Diseases in Polish Cities. Respiratory Treatment and Prevention. Advances in Experimental Medicine and Biology, vol 944. Springer, Cham. 10.1007/5584_2016_55
- Bañeras, J., Ferreira-González, I., Marsal, J. R., Barrabés, J. A., Ribera, A., Lidón, R. M., & García-Dorado, D. (2018). Short-term exposure to air pollutants increases the risk of ST elevation myocardial infarction and of infarct-related ventricular arrhythmias and mortality. International journal of cardiology, 250, 35-42, https://doi.org/10.1016/j.ijcard.2017.10.004
- Bhaduri, B., Bright, E., Coleman, P., & Dobson, J. (2002). LandScan. Geoinformatics, 5(2), 34-37.
- Bigazzi, A. Y., & Figliozzi, M. A. (2013). Marginal costs of freeway traffic congestion with on-road pollution exposure externality. Transportation Research Part A: Policy and Practice, 57, 12-24, https://doi.org/10.1016/j.tra.2013.09.008
- Choma, E. F., Evans, J. S., Hammitt, J. K., Gómez-Ibáñez, & J. A., Spengler, J. D. (2020). Assessing the health impacts of electric vehicles through air pollution in the United States. Environment International, 144, 106015, https://doi.org/10.1016/j.envint.2020.106015
- Cheung, W., M. (2022). A scenario-based approach to predict energy demand and carbon emission of electric vehicles on the electric grid. Environ Sci Pollut Res 29, 77300–77310 (2022). https://doi.org/10.1007/s11356-022-21214-w
- Coudrin, C., & Mariotti, S. (2020). La Réunion facing climatic challenges: observations and the solutions. In: INSEE Report 63 (in French)
- Daudin, V., Lieutier, S., & Besnard, A. (2014) Work commuting : The peri-urbanization versus substainable transports, INSEE Report 4 (in French)
- CE Delft (2020). Health costs of air pollution in European cities and the linkage with transport. CE Delft: Delft, The Netherlands.
- de Palma, A., & Marchal, F. (2002). Real cases applications of the fully dynamic METROPOLIS tool-box: an advocacy for large-scale mesoscopic transportation systems. Networks and spatial economics, 2, 347-369, https://doi.org/10.1023/A:1020847511499
- de Palma, A., Marchal, F., & Nesterov, Y. (1997). METROPOLIS: Modular system for dynamic traffic simulation. Transportation Research Record, 1607(1), 178-184, https://doi.org/10.3141/1607-24
- D'elia, I., Bencardino, M., Ciancarella, L., Contaldi, M., & Vialetto, G. (2009). Technical and Non-Technical Measures for air pollution emission reduction: The integrated assessment of the regional Air Quality Management Plans through the Italian national model. Atmospheric Environment, 43(39), 6182-6189 https://doi.org/10.1016/j.atmosenv.2009.09.003
- Dhondt, S., Beckx, C., Degraeuwe, B., Lefebvre, W., Kochan, B., Bellemans, T., & Putman, K. (2012). Health impact assessment of air pollution using a dynamic exposure profile: Implications for exposure and health impact estimates. Environmental impact assessment review, 36, 42-51, https://doi.org/10.1016/j.eiar.2012.03.004
- Dons, E., Beckx, C., Arentze, T., Wets, G., & Panis, L. I. (2011). Using an activity-based framework to determine effects of a policy measure on population exposure to nitrogen dioxide. Transportation research record, 2233(1), 72-79, https://doi.org/10.3141/2233-09
- Faustini, A., Rapp, R., & Forastiere, F. (2014). Nitrogen dioxide and mortality: review and meta-analysis of long-term studies. European Respiratory Journal, 44(3), 744-753. https://doi.org/10.1183/09031936.00114713
- Fang, D., Wang, Q. G., Li, H., Yu, Y., Lu, Y., & Qian, X. (2016). Mortality effects assessment of ambient PM2. 5 pollution in the 74 leading cities of China. Science of the Total Environment, 569, 1545-1552, https://doi.org/10.1016/j.scitotenv.2016.06.248
- Ferrero, E., Alessandrini, S., & Balanzino, A. (2016). Impact of the electric vehicles on the air pollution from a highway. Applied energy, 169, 450-459, https://doi.org/10.1016/j.apenergy.2016.01.098
- Friedrich, R., & Quinet, E. (2011). External costs of transport in Europe. In A handbook of Transport Economics. Edward Elgar Publishing, https://doi.org/10.4337/9780857930873.00024

- Garrett, P., & Casimiro, E. (2011). Short-term effect of fine particulate matter (PM 2.5) and ozone on daily mortality in Lisbon, Portugal. Environmental Science and Pollution Research, 18, 1585-1592, https://doi.org/10.1007/s11356-011-0519-z
- Hao, J. Y., Hatzopoulou, M., & Miller, E. J. (2010). Integrating an activity-based travel demand model with dynamic traffic assignment and emission models: Implementation in the Greater Toronto, Canada, area. Transportation Research Record, 2176(1), 1-13, https://doi.org/10.3141/2176-01
- Hatzopoulou, M., & Miller, E. J. (2010). Linking an activity-based travel demand model with traffic emission and dispersion models: Transport's contribution to air pollution in Toronto. Transportation Research Part D: Transport and Environment, 15(6), 315-325, https://doi.org/10.1016/j.trd.2010.03.007
- Hayhoe, K., Cayan, D., Field, C. B., Frumhoff, P. C., Maurer, E. P., Miller, N. L., Verville, J. H. (2004). Emissions pathways, climate change, and impacts on California. Proceedings of the national academy of sciences, 101(34), 12422-12427, https://doi.org/10.1073/pnas.0404500101
- Hendrickson, C., & Kocur, G., (1981), Schedule delay and departure time decisions in a deterministic model, Transportation science, 15(1), 62-77, https://doi.org/10.1287/trsc.15.1.62
- Ho, B. Q., Clappier, A., & Blond, N. (2014). Fast and optimized methodology to generate road traffic emission inventories and their uncertainties. CLEAN–Soil, Air, Water, 42(10), 1344-1350, https://doi.org/10.1002/clen.201300261
- Holdway, A. R., Williams, A. R., Inderwildi, O. R., & King, D. A. (2010). Indirect emissions from electric vehicles: emissions from electricity generation. Energy & Environmental Science, 3(12), 1825-1832. https://doi.org/10.1039/C0EE00031K
- Kudoh, Y., Ishitani, H., Matsuhashi, R., Yoshida, Y., Morita, K., Katsuki, S., & Kobayashi, O. (2001). Environmental evaluation of introducing electric vehicles using a dynamic traffic-flow model. Applied Energy, 69(2), 145-159, https://doi.org/10.1016/S0306-2619(01)00005-8
- Lefebvre, W., Degrawe, B., Beckx, C., Vanhulsel, M., Kochan, B., Bellemans, T., & Dhondt, S. (2013). Presentation and evaluation of an integrated model chain to respond to traffic-and health-related policy questions. Environmental modelling & software, 40, 160-170, https://doi.org/10.1016/j.envsoft.2012.09.003
- Martinez, G. S., Spadaro, J. V., Chapizanis, D., Kendrovski, V., Kochubovski, M., & Mudu, P. (2018). Health impacts and economic costs of air pollution in the metropolitan area of Skopje. International journal of environmental research and public health, 15(4), 626, https://doi.org/10.3390/ijerph15040626
- McCubbin, D. R., & Delucchi, M. A. (2003). The health effects of motor vehicle-related air pollution. In Handbook of Transport and the Environment (Vol. 4, pp. 411-427). Emerald Group Publishing Limited, https://doi.org/10.1108/9781786359513-022
- Ntziachristos, L., Gkatzoflias, D., Kouridis, C., & Samaras, Z. (2009). COPERT: a European road transport emission inventory model. In Information Technologies in Environmental Engineering: Proceedings of the 4th International ICSC Symposium Thessaloniki, Greece, May 28-29, 2009 (pp. 491-504). Springer Berlin Heidelberg, 10.1007/978-3-540-88351-7_37
- Observatoire Energie Réunion, Electricity efficiency plan for La Réunion in 2019, 2020 (in French)
- Raeissi, P., Khalilabad., T., H., & Hadian, M. The impacts of fuel price policies on air pollution: case study of Tehran. Environ Sci Pollut Res Int. 2022 Feb;29(8):11780-11789. https://doi.org/10.1007/s11356-021-16550-2
- Rowangould, G. M. (2015). A new approach for evaluating regional exposure to particulate matter emissions from motor vehicles. Transportation research part D: transport and environment, 34, 307-317, https://doi.org/10.1016/j.trd.2014.11.020
- Smit, R., Ntziachristos, L., & Boulter, P. (2010). Validation of road vehicle and traffic emission models–A review and meta-analysis. Atmospheric environment, 44(25), 2943-2953, https://doi.org/10.1016/j.atmosenv.2010.05.022
- Sutton, O. G. (1947). The problem of diffusion in the lower atmosphere. Quarterly Journal of the Royal Meteorological Society, 73(317-318), 257-281, https://doi.org/10.1002/qj.49707331704
- Vallamsundar, S., Lin, J., Konduri, K., Zhou, X., & Pendyala, R. M. (2016). A comprehensive modeling framework for transportation-induced population exposure assessment. Transportation Research Part D: Transport and Environment, 46, 94-113, https://doi.org/10.1016/j.trd.2016.03.009
- Vickrey, W. S. (1969). Congestion theory and transport investment. The American Economic Review, 59(2), 251-260, https://www.jstor.org/stable/1823678
- Vlachokostas, C., Achillas, C., Moussiopoulos, N., Kalogeropoulos, K., Sigalas, G., Kalognomou, E. A., & Banias, G. (2012). Health effects and social costs of particulate and photochemical urban air pollution: a case study for Thessaloniki, Greece. Air Quality, Atmosphere & Health, 5, 325-334, https://doi.org/10.1007/s11869-010-0096-1

- Vosough, S., de Palma, A., & Lindsey, R. (2022). Pricing vehicle emissions and congestion externalities using a dynamic traffic network simulator. Transportation Research Part A: Policy and Practice, 161, 1-24. https://doi.org/10.1016/j.tra.2022.04.017
- Walton, H., Dajnak, D., Beevers, S., Williams, M., Watkiss, P., & Hunt, A. (2015). Understanding the health impacts of air pollution in London. London: Kings College London, Transport for London and the Greater London Authority, 1(1), 6-14.
- Zheng, Y., He, X., Wang, H., Wang, M., Zhang, S., Ma, D., & Wu, Y. (2020). Well-to-wheels greenhouse gas and air pollutant emissions from battery electric vehicles in China. Mitigation and Adaptation Strategies for Global Change, 25, 355-370, https://doi.org/10.1007/s11027-019-09890-5
- Ziska, L. H., & Caulfield, F. A. (2000). Rising atmospheric carbon dioxide and ragweed pollen production: implications for public health. Australian Journal of Plant Physiology, 27, 893-898, https://doi.org/10.1071/PP00032

## Appendix

***A1: Travel demand parameter values***

| Parameter | Value |
|---|---|
| Studied time period | 6:00 a.m. - 12:00 p.m. |
| Length of time period (t) | 20 min |
| Unit cost of travel time (α) | N(10, 2) |
| Desired arrival time ($t^*$) | N(510, 70) |
| Unit cost of early arrival (β) | N(5, 1) |
| Unit cost of late arrival ($\gamma$) | N(8, 1) |
| Width of on-time-arrival window (δ) | 30 |
| Logit scale parameter for auto departure-time choice | 2 |

*This table summarizes the different parameters used for the baseline scenario simulation in METROPOLIS*

***A2: Dispersion parameter values***

| Parameter | Value |
|---|---|
| Wind direction | North-West to South East |
| Wind speed ($u_s$) | 7.4 $m.s^{-1}$ |
| Emitter height (H) | 0.5 m |
| Receptor height (z) | 1.5 m |
| Standard deviation of lateral concentration ($\sigma_y^2(x)$) | $\frac{ax}{(1+bx)^e}$ |
| Standard deviation of vertical concentration ($\sigma_z^2(x)$) | $\frac{dx}{(1+bx)^e}$ |
| a | 0.0787 |
| b | 0.0014 |
| c | 0.135 |
| d | 0.0745 |
| e | 0.465 |

*This table summarizes the different parameters used in the dispersion model*

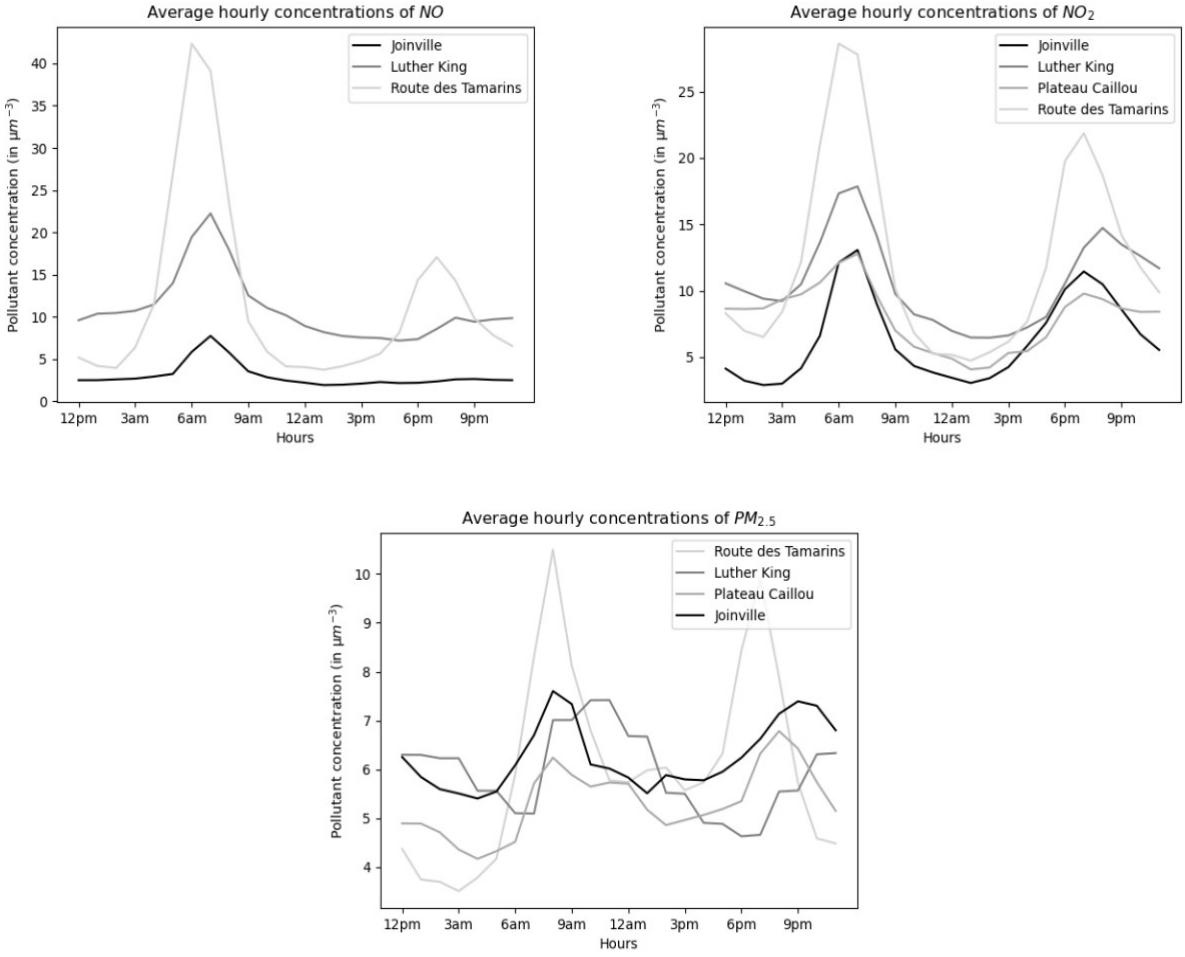


*The hourly average concentrations for the various pollution stations are shown in this graph. The nitrogen monoxide time profile is shown in the top left figure. The temporal profile of nitrogen dioxides is shown on the right. And the bottom figures show the particulate matter time profile. Source: AtmoRéunion*

### *A3: NO, $NO_2$ and $PM_{2.5}$ average hourly concentrations at La Réunion*

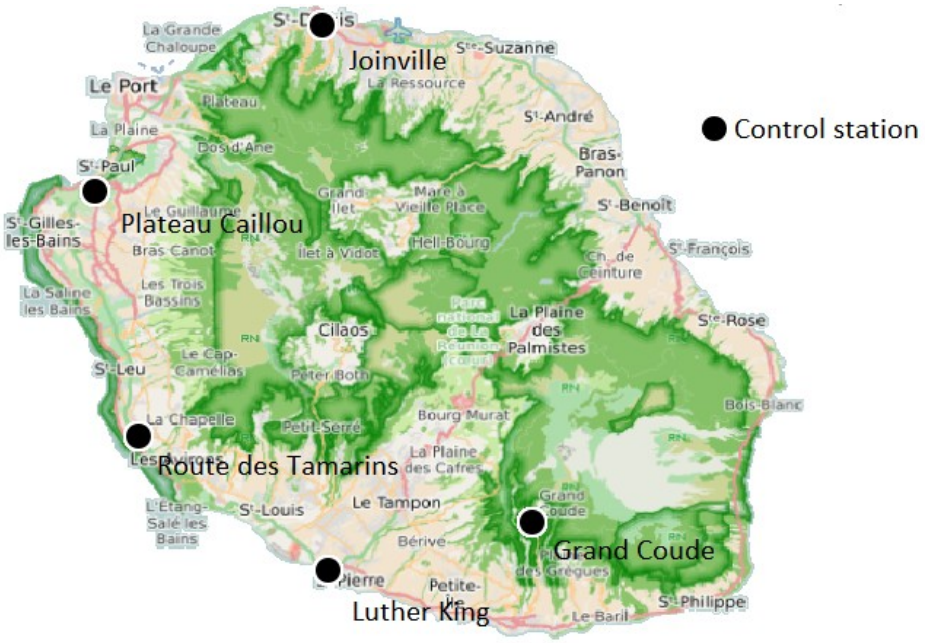


*This map displays the localisation of the different air control stations at La Réunion. Source: AtmoRéunion*

***A4: Map of the different air control stations at La Réunion***